Ore Geology Reviews 53 (2013) 77–92

Contents lists available at SciVerse ScienceDirect

Ore Geology Reviews

journal homepage: www.elsevier.com/locate/oregeorev

Constraints of C–O–S–Pb isotope compositions and Rb–Sr isotopic age on the origin of the Tianqiao carbonate-hosted Pb–Zn deposit, SW China

Jiaxi Zhou [a,b], Zhilong Huang [a,*], Meifu Zhou [b], Xiaobiao Li [a], Zhongguo Jin [a]

[a] State Key Laboratory of Ore Deposit Geochemistry, Institute of Geochemistry, Chinese Academy of Sciences, Guiyang 550002, China
[b] Department of Earth Sciences, University of Hong Kong, Pokfulan Road, Hong Kong, China

ARTICLE INFO

Article history:
Received 31 July 2012
Received in revised form 24 December 2012
Accepted 3 January 2013
Available online 12 January 2013

Keywords:
C–O–S–Pb isotopes
Sulfide Rb–Sr isotopic age
Tianqiao carbonate-hosted Pb–Zn deposit
SW China

ABSTRACT

The Tianqiao Pb–Zn deposit in the western Yangtze Block, southwest China, is part of the Sichuan–Yunnan–Guizhou (SYG) Pb–Zn metallogenic province. Ore bodies are hosted in Devonian and Carboniferous carbonate rocks, structurally controlled by a thrust fault and anticline, and carried about 0.38 million tons Pb and Zn metals grading >15% Pb + Zn. Both massive and disseminated Pb–Zn ores occur either as veinlets or disseminations in dolomitic rocks. They are composed of ore minerals, pyrite, sphalerite and galena, and gangue minerals, calcite and dolomite. $\delta^{34}S$ values of sulfide minerals range from +8.4 to +14.4‰ and display a decreasing trend from pyrite, sphalerite to galena ($\delta^{34}S_{pyrite} > \delta^{34}S_{sphalerite} > \delta^{34}S_{galena}$). We interpret that reduced sulfur derived from sedimentary sulfate (gypsum and barite) of the host Devonian to Carboniferous carbonate rocks by thermal–chemical sulfate reduction (TSR). $\delta^{13}C_{PDB}$ and $\delta^{18}O_{SMOW}$ values of hydrothermal calcite range from −5.3 to −3.4‰ and +14.9 to +19.6‰, respectively, and fall in the field between mantle and marine carbonate rocks. They display a negative correlation, suggesting that CO_2 in the hydrothermal fluid was a mixture origin of mantle, marine carbonate rocks and sedimentary organic matter. Sulfide minerals have homogeneous and low radiogenic Pb isotope compositions ($^{206}Pb/^{204}Pb = 18.378$ to 18.601, $^{207}Pb/^{204}Pb = 15.519$ to 15.811 and $^{208}Pb/^{204}Pb = 38.666$ to 39.571) that are plotted in the upper crust Pb evolution curve and overlap with that of Devonian to Carboniferous carbonate rocks and Proterozoic basement rocks in the SYG province. Pb isotope compositions suggest derivation of Pb metal from mixed sources. Sulfide minerals have $^{87}Sr/^{86}Sr$ ratios ranging from 0.7125 to 0.7167, higher than Sinian to Permian sedimentary rocks and Permian Emeishan flood basalts, but lower than basement rocks. Again, Sr isotope compositions are supportive of a mixture origin of Sr. They have an Rb–Sr isotopic age of 191.9 ± 6.9Ma, possibly reflecting the timing of Pb–Zn mineralization. C–O–S–Pb–Sr isotope compositions of the Tianqiao Pb–Zn deposit indicate a mixed origin of ore-forming fluids, which have Pb–Sr isotope homogenized before the mineralization. The Permian flood basalts acted as an impermeable layer for the Pb–Zn mineralization hosted in the Devonian–Carboniferous carbonate rocks.

1. Introduction

In the western Yangtze Block (Fig. 1A), southwest China, there are about 408 Zn–Pb–(Ag) ore deposits (Liu and Lin, 1999), including the world-class Huize Zn–Pb deposit with 7 million tons (Mt) of Pb and Zn metals (Han et al., 2007a, 2012), five large Pb–Zn deposits with 1 to 3 Mt Pb and Zn metals, namely the Daliangzi, Tianbaoshan, Xiaoshifang, Maoping and Maozu Zn–Pb deposits (Han et al., 2007a, 2012; Liu and Lin, 1999; Wang et al., 2000, 2003, 2010; Zheng and Wang, 1991; Zhou et al., 2001), and more than 40 medium Pb–Zn deposits with 0.2 to 1 Mt Pb and Zn metals, such as the Paoma Zn–Pb deposit (Lin et al., 2010), Lemachang Pb–Zn–Ag deposit (Deng et al., 2000) and Tianqiao Zn–Pb deposit (Zhou et al., 2011). All these deposits, which form the important Sichuan–Yunnan–Guizhou (SYG) Pb–Zn metallogenic province, contain total Pb and Zn metals of more than 20 Mt at grades of >15% Pb + Zn (Table 1), and have been the major source of base metals in China in the past several decades (Cromie et al., 1996; Liu and Lin, 1999). However, origin of these deposits and the mechanism for such giant accumulations of Pb and Zn have long been controversial (Chen, 1986; Deng et al., 2000; Han et al., 2007a, 2012; Hu and Zhou, 2012; Huang et al., 2010; Liao, 1984; Liu and Lin, 1999; Tu, 1984; Xie, 1963; Zheng and Wang, 1991; Zhou et al., 2001, 2011).

The Pb–Zn deposits in the SYG province are hosted in the Late Sinian, Devonian, Carboniferous and early Permian carbonate rocks. A close association of these deposits with the Permian Emeishan flood basalts led Xie (1963) to classify them as distal magmatic-hydrothermal deposits. Evidence linking mineralization to basaltic magmatism includes the occurrence of one hidden Zn–Pb vein in basalt at Xuanwei County of NE Yunnan province. On the other hand, Liao (1984) proposed diverse sources for the ore-forming metals and postulated that all Zn–Pb–(Ag) deposits in NE Yunnan and NW

* Corresponding author. Tel.: +86 851 5895900; fax: +86 851 5891664.
E-mail address: huangzhilong@vip.gyig.ac.cn (Z. Huang).

0169-1368/$ – see front matter © 2013 Elsevier B.V. All rights reserved.
http://dx.doi.org/10.1016/j.oregeorev.2013.01.001

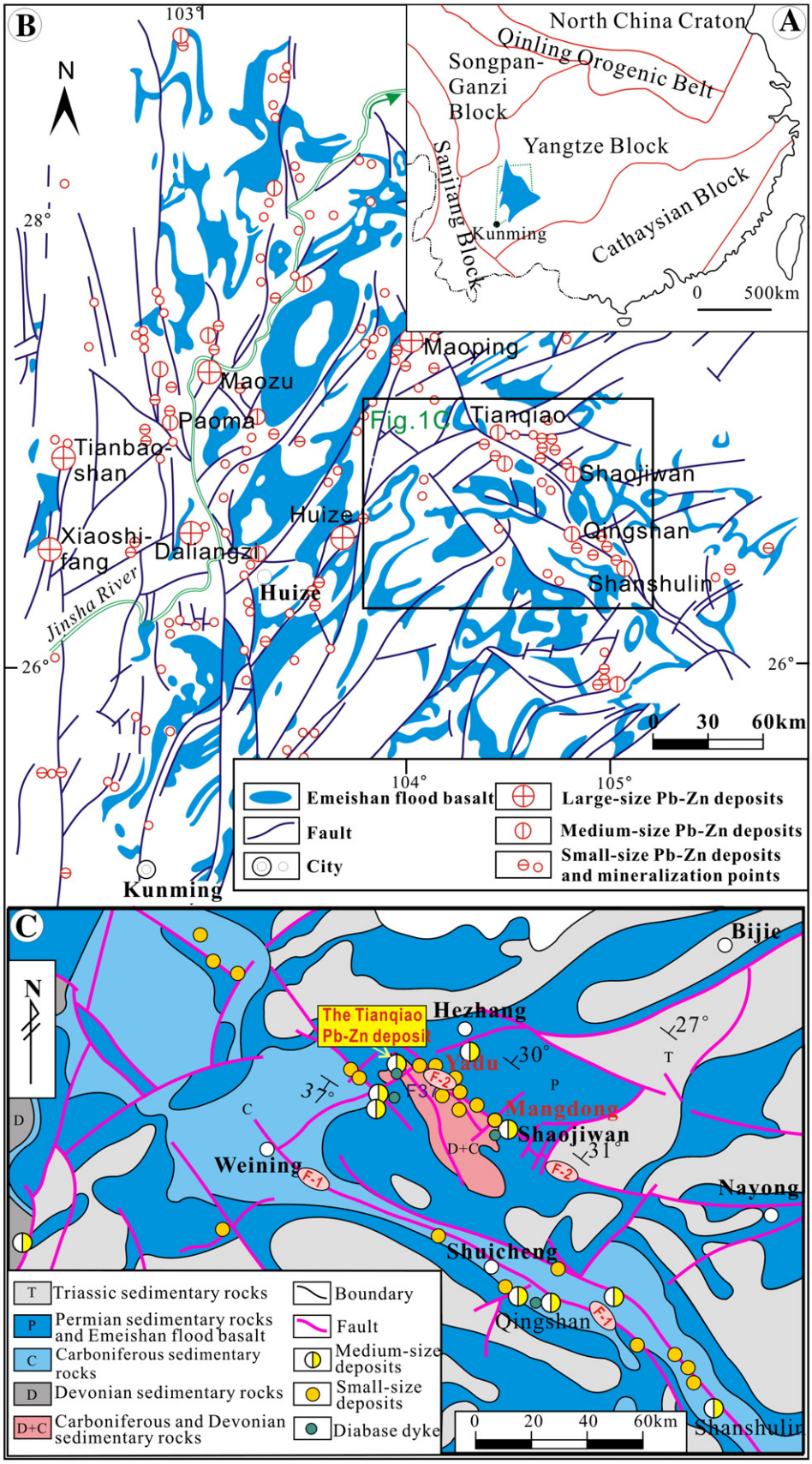

Fig. 1. Regional geological map. Panel A: Tectonic geological sketch drawing; Panel B: Regional geological map of the SYG Pb–Zn metallogenic province, SW China, showing the distribution of Permian Emeishan flood basalts and Pb–Zn deposits (modified from Huang et al., 2010); Panel C: Geological map of the southeastern SYG metallogenic province. (Modified from Jin, 2008).

Table 1
Host strata, locality, tonnage and grade of typical Pb–Zn deposits in the SYG province, SW China.

Name	Host strata	Geographic locality	Metals association	Tonnage and grade
Huize	Carboniferous	26.640147, 103.725219	Zn–Pb–Ge–Cd–Ag	7 Mt, 30–35 wt.% Pb + Zn
Maozu	Sinian	27.356944, 102.989722	Zn–Pb–Cd–Ag	2 Mt, 12–14 wt.% Pb + Zn
Maoping	Devonian–Carboniferous	27.521667, 103.991667	Zn–Pb–Ag	3 Mt, 25–30 wt.% Pb + Zn
Fule	Permian	25.368056, 104.398056	Zn–Pb–Cd–Ge–Ga–In	0.6 Mt, 15–20 wt.% Pb + Zn
Tianbanshan	Sinian	27.075833, 102.408056	Zn–Pb–Cd–Ag	2.6 Mt, 10–15 wt.% Pb + Zn
Daliangzi	Sinian	27.113611, 102.742500	Zn–Pb–Ge–Cd–Ga–Ag	4.5 Mt, 10–12 wt.% Pb + Zn
Xiaoshifang	Sinian	26.503889, 102.106389	Zn–Pb–Cd–Ag	>1 Mt, >15 wt.% Pb + Zn
Yinchanggou	Sinian	27.127500, 102.792500	Zn–Pb–Ag	>0.3Mt, >14 wt.% Pb + Zn
Paoma	Sinian	27.204639, 102.824972	Zn–Pb	>0.2 Mt, >10 wt.% Pb + Zn
Tianqiao	Devonian–Carboniferous	27.062222, 104.564722	Zn–Pb–Cd–Ag–Ge	0.4 Mt, 15–18 wt.% Pb + Zn
Yinchangpo	Carboniferous	26.800833, 103.706944	Pb–Zn–Ag–Ge	>0.2 Mt, >20 wt.% Pb + Zn
Shanshulin	Carboniferous	26.495278, 105.025000	Zn–Pb–Ag–Cd–As	>0.5 Mt, >20 wt.% Pb + Zn
Shaojiwan	Devonian	27.473611, 103.941389	Zn–Pb–Cd–Ag	0.5 Mt, 15–20 wt.% Pb + Zn
Maomaochang	Carboniferous	26.973333, 104.328611	Zn–Pb–Cd–Ag	>0.3 Mt, >12 wt.% Pb + Zn
Zhazichang	Carboniferous	26.959444, 104.502222	Zn–Pb–Cd–Ag	>0.2Mt, >10 wt.% Pb + Zn
Qingshan	Carboniferous	26.532942, 104.883917	Zn–Pb–Cd–Ag–In	>0.3 Mt, >15 wt.% Pb + Zn
Yadu	Permian	26.991944, 104.710278	Zn–Pb–Cd–Ag	>0.5 Mt, >15 wt.% Pb + Zn
Mangdong	Devonian	26.933889, 104.780833	Zn–Pb–Cd–Ag	>0.3 Mt, >15 wt.% Pb + Zn

Note: The Huize and Maoping Pb–Zn deposit from Han et al. (2007a, 2012) and Zhou et al. (2001), the Maozu, Fule, Tianbanshan, Daliangzi, Xiaoshifang and Yinchanggou Pb–Zn deposit from Liu and Lin (1999), Wang et al. (2000, 2003, 2010), and Zheng and Wang (1991), other Pb–Zn deposits are from Jin (2008), Zhou et al. (2011) and this study.

Guizhou were formed in hydrothermal–sedimentary processes. In the 1980s, Tu (1984) interpreted them as strata-bound ore deposits and proposed that they were generated during hydrothermal reworking of sedimentary rocks. This view was once popular in the 1980's and 1990's (e.g. Chen, 1986; Wang, 1994). Some Pb–Zn deposits in the region were later re-interpreted to be typical Mississippi valley-type (MVT) deposits (e.g. Wang et al., 2000, 2003, 2010; Zheng and Wang, 1991; Zhou et al., 2001). The Emeishan flood basalts have also been considered to be an important source of the ore-forming metals and heat (e.g. Guan and Li, 1999; Han et al., 2007a, 2012; Huang et al., 2003, 2004, 2010; Liu and Lin, 1999). However, despite many investigations and the large number of publications in Chinese, it is still unclear how these metals became so highly concentrated in the region. A widely accepted genetic model for the regional Pb–Zn mineralization is still not available (Han et al., 2012), largely due to the lack of precise ages of the mineralization.

In the southeastern SYG province, there are about 120 Pb–Zn deposits and mineralization, most of which are distributed along NW-trending Weining–Shuicheng (F-1) and Yadu–Mangdong (F-2) faults (Fig. 1C). Although no large, world-class deposits occur in this district, there are at least nine medium deposits and many smaller ones (Fig. 1C). Previous studies are only available in the Chinese literature but have documented that all these deposits occur in Devonian to Permian dolomitic limestone (e.g. Chen, 1986; Jin, 2008; Mao et al., 1998, 2001; Wang et al., 1996; Zhou et al., 2010a, 2010b, 2011). The Tianqiao medium-size Pb–Zn deposit along the Yadu–Mangdong fault (Fig. 1C) has been mined for over a past decade (Jin, 2008). Jin (2008) and Wang et al. (1996) examined the geology of this deposit and thought that the Tianqiao deposit is representative of all the deposits in this district, and considered it to be a sediment-reworked deposit related to the host carbonate rocks and the thrust-fold structure (Fig. 2).

Isotope geochemistry is a powerful tool for the study of hydrothermal deposits, particularly for determining sources of ore-forming fluids and metals. C, O and S isotopes have been widely used to constrain the origin of hydrothermal deposits (e.g. Han et al., 2007a;

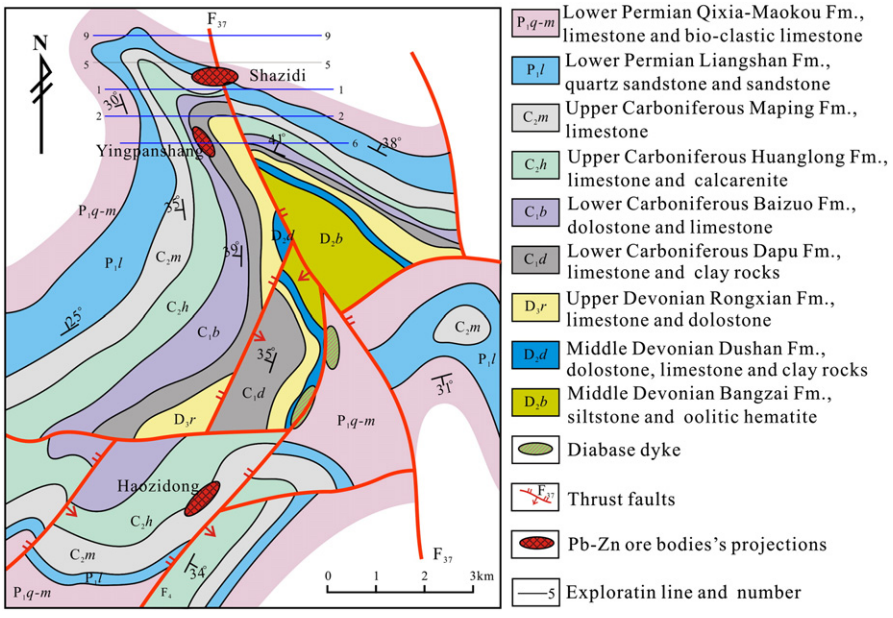

Fig. 2. Geological map of the Tianqiao Pb–Zn deposit.
Modified from Jin (2008).

Huang et al., 2010; Huston et al., 1995; Ohmoto and Goldhaber, 1997; Pfaff et al., 2010; Recio et al., 1997). Pb and Sr isotopes are useful for determining sources of hydrothermal fluids and flow pathways (e.g. Carr et al., 1995; Haest et al., 2010; Herlec et al., 2010; Wilkinson et al., 2005; Zhou et al., 2001). Multiple isotopic studies of the Tianqiao Pb–Zn deposit are not available, but may provide important insights into the genesis of the deposit.

In this paper, we describe the geology of the Tianqiao Pb–Zn deposit and report new C–O isotope for hydrothermal calcite, S–Pb isotope of sulfide, and whole-rock Pb isotope of the wall rocks and Rb–Sr isotopic age of sulfide minerals. These new datasets, together with our previously published results are utilized to constrain the sources of the ore-forming fluids and metals, and age of the Pb–Zn mineralization. We propose an integrated genetic model for the deposit, and discuss the implications of our study for the giant Pb–Zn accumulation in the SYG province.

2. Geological background

2.1. Regional geology

South China is made up of the Yangtze Block to the northwest and the Cathaysian Block to the southeast (Fig. 1A). To the north, the late Paleozoic and early Mesozoic Central Orogenic Belts lie between the Yangtze Block and the North China Craton. To the west, the Yangtze Block is bounded by the Tibetan Tectonic Domain. There are sparse ~2.9 to ~3.3 Ga metamorphic rocks in the northern part of the Yangtze Block, which may represent the crystalline basement (Gao et al., 2011; Qiu et al., 2000). Abundant Archean to Paleoproterozoic detrital zircon grains are recently reported from Meso- to Neoproterozoic sedimentary sequences (Sun et al., 2008, 2009; Wang et al., 2012; Zhao et al., 2010), which are considered to represent the folded basement (Yan et al., 2003). These rocks are well-bedded greywackes, slates and carbonaceous to siliceous sedimentary rocks that are tightly folded but only weakly metamorphosed. In the western Yangtze Block, the folded sedimentary sequences include the ~1.7 Ga Dongchuan and ~1.1 Ga Kunyang Groups and equivalents (Sun et al., 2009; Zhao et al., 2010). They are intruded by abundant Neoproterozoic mafic–ultramafic and felsic intrusions (Wang et al., 2012; Zhou et al., 2002a).

The cover sequences of the western Yangtze Block consist mainly of Paleozoic and Lower Mesozoic strata of shallow marine origin (Yan et al., 2003). The Cambrian strata are composed of black shale, sandstone and limestone interbedded with dolostone. The overlying Ordovician sequences consist of thick-bedded limestone interlayered with dolostone and argillaceous siltstone, which in turn, are overlain by Lower and Middle Silurian shale and fine-grained sandstone. Middle and Upper Devonian rocks are sandstone, siltstone and sandy shale, overlain by Carboniferous clastic rocks and limestone. Permian strata are composed of carbonate rocks and basalts, whereas Triassic rocks include thin limestone layers interlayered with marls and shale. Jurassic, Cretaceous and Cenozoic strata are entirely continental facies (Liu and Lin, 1999).

A major feature of the western Yangtze Block is the mantle plume-derived Emeishan Large Igneous Province covering an area of more than 250,000 km^2 (Fig. 1B; Chung and Jahn, 1995; Zhou et al., 2002b). This igneous province is dominantly composed of volcanic rocks known as Emeishan flood basalts interlayered with Permian limestone. The province also includes numerous mafic–ultramafic intrusions along major faults, some of which host magmatic sulfide or oxide deposits (Zhou et al., 2008).

2.2. Geology of the SYG metallogenic province

The Pb–Zn deposits in the western Yangtze Block are distributed in a large triangular area of 170,000 km^2 in NE Yunnan, NW Guizhou and SW Sichuan (Liu and Lin, 1999). This area represents the eastern part of the Emeishan Large Igneous Province and contains abundant, well-exposed Emeishan flood basalts (Fig. 1B). Both Upper Paleozoic and Lower Mesozoic sedimentary strata are also exposed within the SYG province.

There are more than four hundred Pb–Zn deposits in this province (Liu and Lin, 1999). They are characterized by irregular ore bodies with simple mineralogy, weak wall rock alteration, and high Pb + Zn grade of ores (e.g. Zheng and Wang, 1991; Zhou et al., 2001), usually associated with Ag, Ge, Cd, Ga and In (e.g. Han et al., 2007a; Zhou et al., 2011). They are hosted in carbonate or rarely siliceous carbonate rocks of the Upper Sinian Deying Formation, Devonian Rongxian Formation and Carboniferous Baizuo, Maping and Huanglong Formations and the Lower Permian Qixia Formation (Huang et al., 2004; Jin, 2008; Liu and Lin, 1999). Deposits in the west have the older country wall-rocks than those in the east (e.g. Zheng and Wang, 1991; Zhou et al., 2001, 2011). Notably the host strata are all below the Lower Permian Emeishan flood basalts (e.g. Huang et al., 2004, 2010). Fault systems within the SYG province are very complex and control the distribution of the Pb–Zn deposits. Most faults in the western part of the province are trend NS, whereas those in the east are trend NE and NW (Fig. 1B and C).

2.3. Local geology

In this district, the cover sequences include Devonian, Carboniferous, Permian and Triassic sedimentary strata (Fig. 1C), and Permian Emeishan flood basalts. Diabase dykes locally present may be part of the Emeishan Large Igneous Province which also occur in this district (Fig. 1C).

The Devonian strata consist of sandstone and siltstone in the lower part, and limestone and dolostone in the upper part, whereas the Carboniferous strata are composed of shale and limestone in the lower part and limestone and dolostone in the upper part. The early Permian sequence consists of sandstone, shale, coal layers and limestone, all overlain by Permian Emeishan flood basalts. The basalts, in turn, are overlain by Late Permian sandstone, siltstone and coal measures. The Triassic strata consist of siltstone, sandstone, dolostone and limestone.

NW- and NE-striking faults are well developed. The Pb–Zn deposits are mainly located along the NW-trending tectonic system (Fig. 1C). Pb–Zn ore bodies are hosted in Devonian to Lower Permian dolostone and limestone, mostly in Lower Carboniferous carbonate rocks. A few ore bodies are also hosted in the Upper Devonian, Upper Carboniferous and Lower Permian carbonate rocks. Only sporadic mineralization was observed in the Middle Devonian carbonate rocks (Fig. 1C).

3. Geology of the Tianqiao deposit

3.1. Geology of the Tianqiao mining district

The Tianqiao Pb–Zn deposit is located northwest of the Yadu–Mangdong fault (Fig. 1C). In the Tianqiao mining district, Devonian, Carboniferous and Permian strata form the Tianqiao anticline, which is crosscut by N-, NE- and E-trending faults (Fig. 2). The Devonian sequence includes the Middle Devonian Dushan and Bangzai Formations and the Upper Devonian Rongxian Formation. The Bangzai Formation consists of siltstone and quartz sandstone with lens and lumps of oolitic hematite, whereas the Dushan Formation is made up of thick-layered fine to coarsely crystalline dolostone, dolomitic banded limestone and thin-bedded claystone. The Rongxian Formation is composed of thick-layered, micritic limestone, clayey limestone, pebble limestone and medium to coarsely crystalline dolostone. The Carboniferous strata include the Lower Carboniferous Dapu and Baizuo Formations, Upper Carboniferous Huanglong and Maping Formations, all of which consist chiefly of limestone and dolostone with minor claystone. The overlying Lower Permian strata consist of limestone

of the Qixia and Maokou Formations, and quartz sandstone and argillaceous sandstone of the Liangshan Formation (Fig. 2).

The Tianqiao anticline has the axial plane that strikes N45–60W and both limbs roughly with the same strike but dipping NE and SW with dipping angles mostly of 30–45°. The Lower Devonian Danlin Formation forms the core of the Tianqiao anticline, and limbs contain Middle–Upper Devonian, Carboniferous and Permian carbonate rocks. Being the largest fault in the mining district, F_{37} crosscuts the Tiaoqiao anticline (Figs. 2 and 3). This fault is 14 km long and is marked by a 1 to 6 m wide shear zone. It strikes N50–90° E and dips 50–70° to NE. Movement along the fault is oblique with 20 to 60 m of vertical displacement and 80 to 240 m of horizontal displacement. The relationship between the Tianqiao anticline and the F_{37} thrust fault was considered to be synchronous and similar to other thrust-fold tectonic systems in the SYG province (Han et al., 2012).

3.2. Pb–Zn mineralization style

Major ore bodies occur in dolomitic limestone and dolomite of the Lower Carboniferous Datang and Baizuo Formations, which form the NW-trending nose of the plunging anticline, and are located along the fault F_{37} (Figs. 2 and 3). Thirty-two ore bodies occur in the limbs of the Tianqiao anticline where they form the Yingpanshang and Shazidi ore clusters, near the axis in the northeastern and southern limbs, respectively (Fig. 2). Underground mining and exploratory drilling in these two clusters provide excellent access to the ore-bodies. Another ore cluster, known as the Haozidong ore cluster, occurs in the southwestern limb of the anticline, well away from the axis (Fig. 2). Ore bodies in this cluster are poorly exposed, but strongly oxidized near the surface. Thus primary ores are not available.

Fifteen ore bodies are recognized in the Yingpanshang cluster, the largest of which is 200 m long, 100 m wide and 1.3 to 1.8 m thick. Ores in this body have an average grade of 1.23 wt.% Pb and 15.69 wt.% Zn. The Shazidi cluster comprises 17 ore bodies. Two relatively large bodies are 250 m long, 120 m wide and 1.4 to 1.9 m thick and 320 m long, 220 m wide and 1.7 to 5.2 m thick, respectively. Ores from these two clusters have significantly variable Pb ranging from 0.04 wt.% to 7.32 wt.% and Zn from 0.49 wt.% to 26.7 wt.% (Jin, 2008). They have higher Zn than Pb with Zn/Pb ratios mostly of 5 to 10, with the exception of two ore bodies from the Shazidi cluster that have higher Pb than Zn. The ores from the Tianqiao deposit contain small amounts of Ge, Ga, Cd and Ag. These trace metals are thought to be hosted in sphalerite and galena (Zhou et al., 2011). The immediate hosting rocks of the ore bodies are dolomitic limestone of the upper part of the Dapu Formation and dolomite of the middle–upper part of the Baizuo Formation (Fig. 2). Ore bodies are strata-bounded as tabular and lenticular bodies with sharp boundaries against the wall rocks (Fig. 3). Some ore bodies contain galena, sphalerite and pyrite veinlets hosted in limestone and dolomite. Banded ores consist of alternating layers rich in ore minerals or calcite.

Pb–Zn ores of the Tianqiao deposit are highly oxidized near the surface and primary ores are preserved only at depth of more than 120 m. Oxidized ores have extremely complex mineral assemblages, including acrusite, anglesine, siderite, smithsonite, calamine, hydrozinkite, antunesite and malachite (Jin, 2008). Primary ores are massive, disseminated or banded (Fig. 4A and C–F), and are composed of sphalerite, galena and pyrite, with calcite and dolomite as gangue minerals. Small amounts of chalcopyrite, quartz and fluorite are also commonly present.

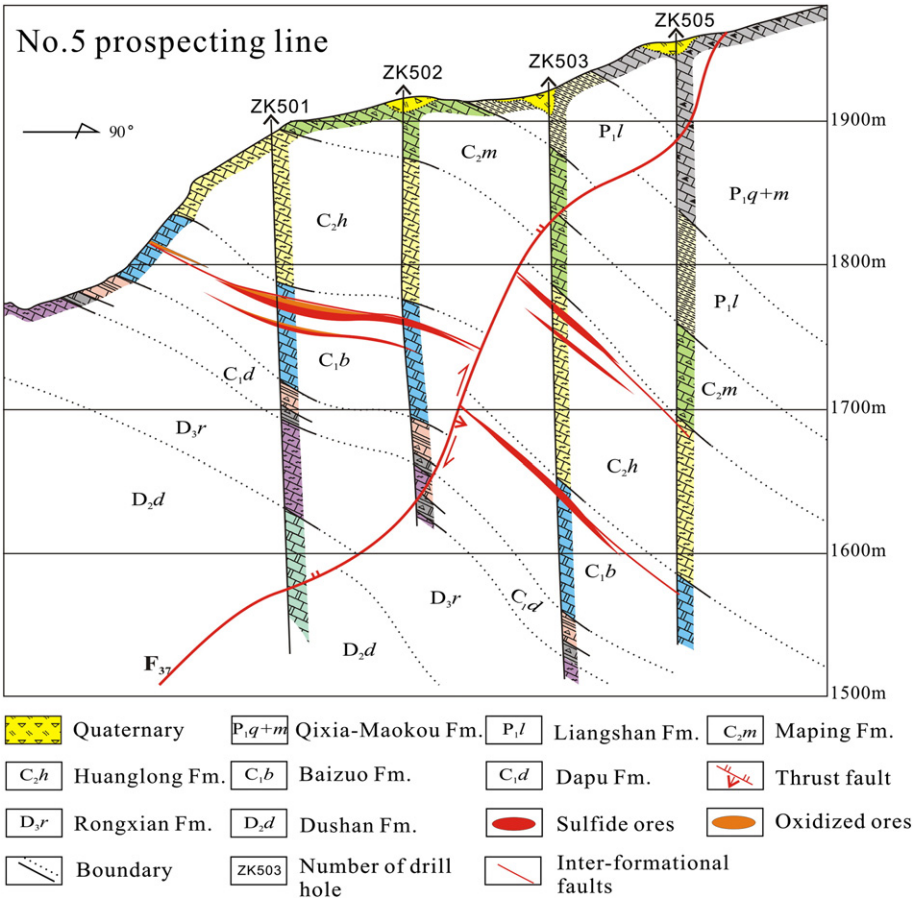

Fig. 3. Cross-section of No. 5 prospecting line of the Tianqiao Pb–Zn deposit.

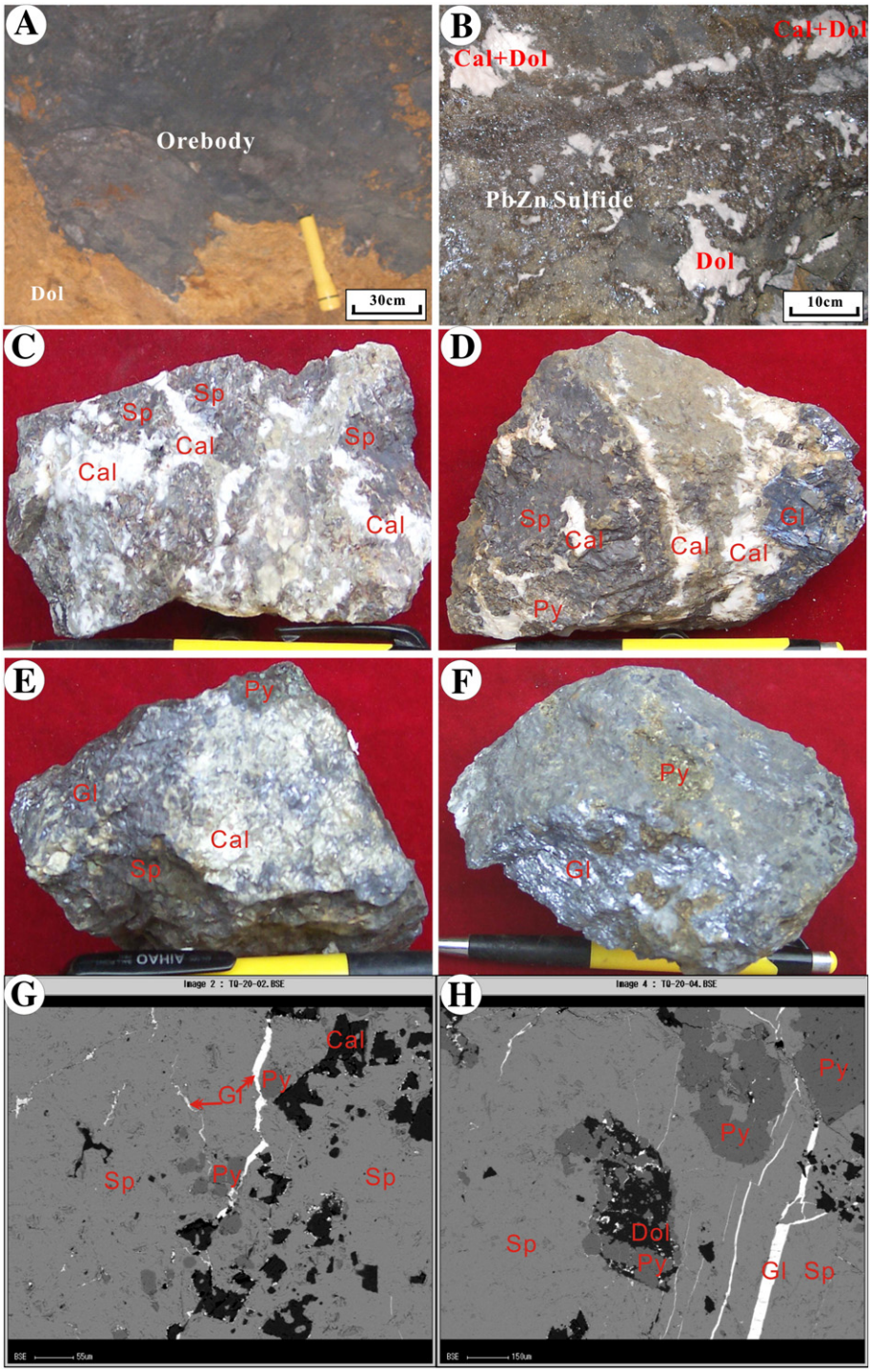

Fig. 4. Field photos of ore bodies and wall rocks of the Tianqiao Pb–Zn deposit. A: The primary ore body in coarse-grained dolostone of the Lower Carboniferous Dapu Fm., and the distinctive boundary between the ore body and wall rocks; B: the gangue calcites and dolomites in primary ores; C: fine- to coarse-grained sphalerite (Sp) + lumpy, patch and vein calcite (Cal); D: fine- to coarse-grained Sp + patch and vein Cal + coarse-grained pyrite (Py); E: coarse-grained Py + patch Cal + fine- to coarse-grained Sp + granular and corrugated Galena (Gl); F: subhedral and framboidal Py + granular and corrugated Gl; G: coarse-grained Sp + vein Gl + cubic Py + calcite; H: coarse-grained Sp + Py + dolomite (Dol) + vein Gl.

3.3. Paragenetic sequence of mineralization and alteration

Ores from the Tianqiao deposit have experienced diagenetic, hydrothermal and oxidized periods. The hydrothermal period is composed of sulfide-carbonate and carbonate stages. There are three principal mineral assemblages formed in the sulfide-carbonate stage (Fig. 5). In the sphalerite–pyrite–dolomite assemblage, sphalerite is fine- to coarse-grained (0.08–12 mm) with xenomorphic to automorphic granular textures (Fig. 4B, C). It is dark brown and occurs as massive, porphyritic and banded forms or in disseminated aggregates. Individual grains are commonly skeletal but have well-developed cleavage. Pyrite is also coarse-grained (2–5 mm), has both octahedral and cubic forms and commonly occurs as disseminations or bands in the wall-rocks adjacent to the ores (Fig. 4B). Dolomite is lumpy and patch (Fig. 4B, C), about 10 cm in size. In the sphalerite–pyrite–galena–calcite assemblage, sphalerite is fine- to coarse-grained (0.05–10 mm) with xenomorphic

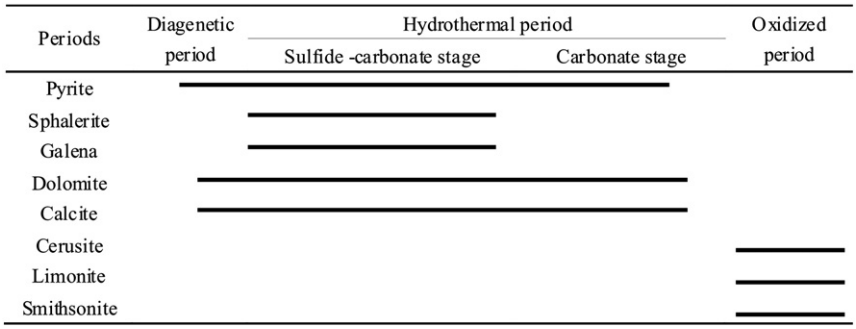

Fig. 5. Mineral assemblages in the paragenetic sequence of the Tianqiao Pb–Zn deposit.

to automorphic granular textures (Fig. 4D, E). It occurs in massive and banded forms or in disseminated aggregates and is brown yellow in color. Associated pyrite is also coarse-grained (2–5 mm), has both octahedral and cubic forms and commonly occurs as disseminations or bands in the wall-rocks adjacent to the ores (Fig. 4E). Galena has a granular and corrugated texture (Fig. 4D, E). Individual grains are 0.1 to 15 mm in diameter, have cubic cleavage and show obvious deformation. Calcite is patch (Fig. 4C, E), about 6 cm. In the sphalerite–galena–calcite assemblage, light yellow sphalerite is fine-grained (0.01–1 mm) with xenomorphic granular textures. It occurs in banded forms or in disseminated aggregates. Galena formed in this stage occurs as veins (Fig. 4F–H) filling in the previous formed sphalerite. Calcite occurs as fine veins (Fig. 4B–D).

Prior to the mineralization, carbonate minerals formed and associated with pervasive alteration of the wall rocks adjacent to ores where they occur as veins and vein networks. This alteration is thought to

Table 2
Sulfur isotope compositions of the Tianqiao Pb–Zn deposit.

Sample no.	Geographic locality	Mineral	$\delta^{34}S$/‰	Source
TQ-3-1	27.0622, 104.5647	Galena	9.8	Zhou et al. (2010a)
TQ-3-2		B-Sphalerite	14.0	
TQ-10		B-Sphalerite	13.7	
TQ-13-1		Galena	9.3	
TQ-13-2		L-Sphalerite	11.7	
TQ-16		Y-Sphalerite	13.7	This paper
TQ-18-1		Pyrite	13.7	
TQ-18-2		Y-Sphalerite	13.1	
TQ-19		Pyrite	14.4	
TQ-23		Pyrite	12.8	
TQ-24-1		Pyrite	12.9	Zhou et al. (2010a)
TQ-24-2		Galena	8.9	
TQ-24-3		B-Sphalerite	12.3	
TQ-24-4		Y-Sphalerite	11.9	
TQ-24-5		L-Sphalerite	10.9	
TQ-25-1		Galena	8.5	
TQ-25-2		L-Sphalerite	12.1	
TQ-52		Galena	8.4	This paper
TQ-54-1		Galena	8.4	
TQ-54-2		Y-Sphalerite	12.2	
TQ-60-1		Pyrite	13.2	
TQ-60-2		Y-Sphalerite	12.4	
TQ-65		Galena	8.7	
HTQ-T1S1	27.0585, 104.5709	Sphalerite	11.5	Gu (2007)
HTQ-T1S2		Galena	11.1	
HTQ-T2S1		Galena	12.6	
HTQ-T2S2		Sphalerite	14.2	
HTQ-T3S1		Sphalerite	12.4	
HTQ-T3S2		Galena	10.7	
HTQ-T5S		Galena	11.0	
HTQ-T6S1		Sphalerite	11.6	
HTQ-T6S2		Galena	11.4	
HTQ-T4S1		Sphalerite	11.5	
HTQ-T4S2		Galena	11.9	
HTQ-T7S		Pyrite	13.4	
Tian-1	27.0622, 104.5647	Sphalerite	12.9	Jin (2008)
Tian-2		Galena	9.4	

Note: Sample no. Q-3-1 and TQ-3-2 are selected from the same as sample, TQ-13-1 and TQ-13-2 from the same as sample, TQ-18-1 and TQ-18-2 from the same as sample, TQ-24-1, TQ-24-2, TQ-24-3, TQ-24-4 and TQ-24-5 from the same as sample, TQ-25-1 and TQ-25-2 from the same as sample, TQ-54-1 and TQ-54-2 from the same as sample. B-Sphalerite is brown sphalerite, Y-Sphalerite is brownish-yellow sphalerite and L-Sphalerite is light yellow sphalerite. Analytical uncertainty is 2σ.

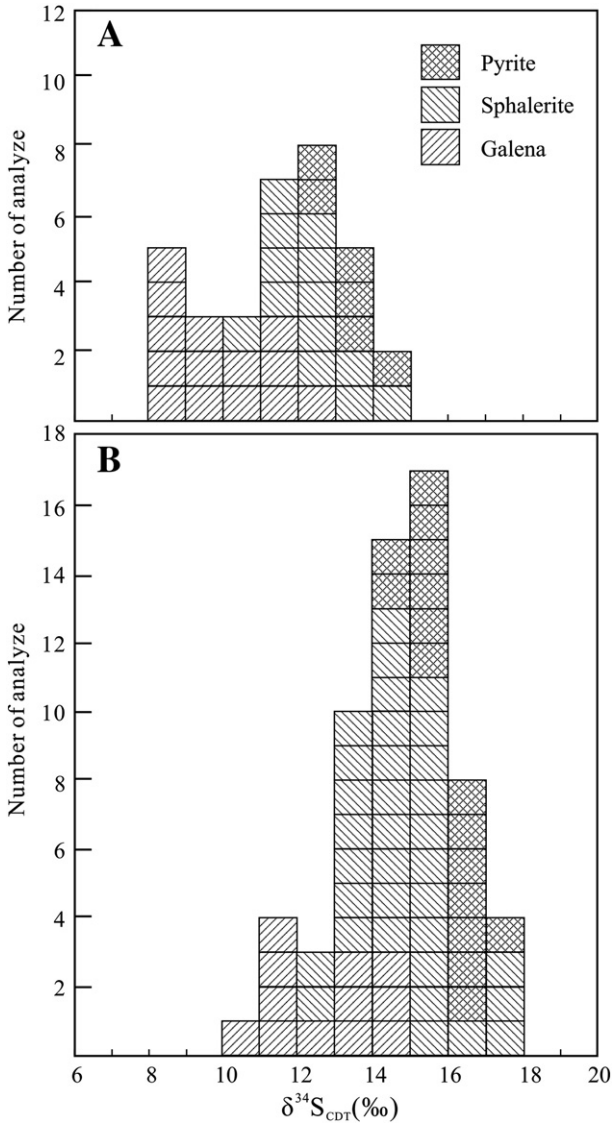

Fig. 6. S isotope compositions histogram of the Tianqiao Pb–Zn deposit (A) and the world-class Huize Pb–Zn deposit (B). S isotope compositions of the Huize deposit are taken from Han et al. (2007a), Li et al. (2007b), and Liu and Lin (1999).

have played a major role in mineralization by increasing the porosity of the wall rocks by as much as 10% (Jin, 2008). As a result of dolomitization, geode and pore were generated enhancing the brittleness of the rocks and leading to increased fracturing. Spaces are thus provided for mineralization by infilling and replacement.

4. Analytical methods

Samples were collected from different stages and positions of the Tianqiao Pb–Zn deposit, and were crushed to 40–80 meshes. Pyrite, sphalerite, galena and calcite were handpicked from the ore samples under a binocular microscope. The purity of single mineral separate was more than 99%. All mineral separates were cleaned in an ultrasonic bath before being powdered in an agate mortar. Sphalerite, galena and pyrite separates were analyzed for S–Pb isotope compositions, sphalerite and pyrite separates for Rb–Sr isotopic dating, and calcite separates for C–O isotope compositions.

S isotope analyses of sulfide minerals were carried out at the State Key Laboratory of Environmental Geochemistry, Institute of Geochemistry, Chinese Academy of Sciences, by using Continuous Flow Mass Spectrometer. GBW 04415 and GBW 04414 Ag_2S were used as the external standards, and the relative errors (2σ) were better than 0.1‰ from the replication of standard materials. Sulfur isotopic compositions are reported relative to CDT.

C–O isotope compositions were obtained using MAT-251 EM mass spectrometer at the Chinese Academy of Geological Sciences. Calcite reacts with pure phosphoric acid to produce CO_2. The analytical precisions (2σ) are ±0.2‰ for carbon isotope and ±2‰ for oxygen isotope. C–O isotope compositions are reported relative to PDB. $\delta^{18}O_{SMOW} = 1.03086 \times \delta^{18}O_{PDB} + 30.86$ (Friedman and O'Neil, 1977).

Pb isotope analyses were carried out by using the GV Isoprobe-T Thermal Ionization Mass Spectrometer at the Beijing Institute of Uranium Geology. The analytical procedure involved dissolution of samples using HF and $HClO_4$ in crucibles, followed by basic anion exchange resin to purify Pb. Analytical results for the standard NBS 981 are $^{208}Pb/^{204}Pb = 36.611 \pm 0.004$ (2σ), $^{207}Pb/^{204}Pb = 15.457 \pm 0.002$

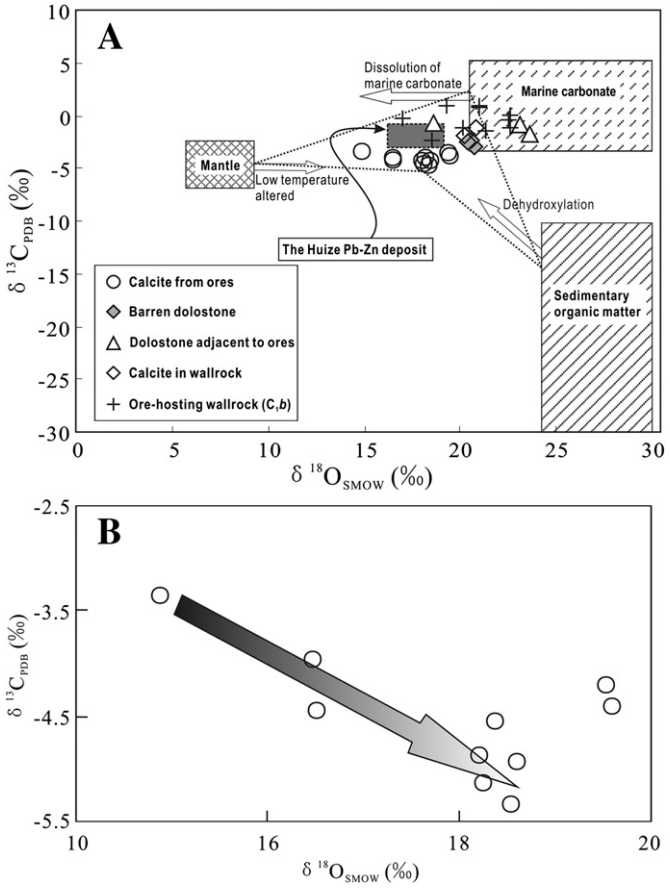

Fig. 7. Plots of $\delta^{13}C_{PDB}$ vs. $\delta^{18}O_{SMOW}$ for the Tianqiao Pb–Zn deposit. C and O isotopic compositions of the Huize deposit are taken from Han et al. (2007a), Huang et al. (2010) and Li et al. (2007b).

Table 3
C and O isotope compositions of the Tianqiao Pb–Zn deposit.

Sample no.	Object	Geographic locality	Description	$\delta^{13}C_{PDB}$/‰	$\delta^{18}O_{PDB}$/‰	$\delta^{18}O_{SMOW}$/‰	Source
TQ-10	Calcite	27.0622, 104.5647	Sp-Ga-Py ore	−4.6	−12.1	18.4	This paper
TQ-13	Calcite		Sp-Ga-Py ore	−4.2	−11.0	19.6	
TQ-48	Calcite		Sp-Ga-Py ore	−4.9	−12.3	18.2	
TQ-50	Calcite		Sp-Ga-Py ore	−4.0	−14.0	16.5	
TQ-57	Calcite		Sp-Ga-Py ore	−5.3	−12.0	18.6	
TQ-70	Calcite		Sp-Ga-Py ore	−5.1	−12.2	18.3	
TQ-08-01	Calcite		Sp-Ga-Py ore	−3.4	−15.5	14.9	
TQ-08-02	Calcite		Sp-Ga-Py ore	−4.9	−11.9	18.6	
TQ-08-03	Calcite		Sp-Ga-Py ore	−4.4	−13.9	16.5	
HTQ-1	Dolostone	27.0585, 104.5709	Immediate wall rock	−3.0	−9.9	20.7	Mao (2000)
HTQ-2	Dolostone		Barren wall rock	−0.8	−7.6	23.1	
Ave. value	Limestone		Barren wall rock	−1.8	−7.1	23.6	Zhang et al. (1998)
Tian-1	Calcite		Calcite vein in wall rock	−1.2	−9.9	20.8	Wang et al. (1996)
Tian-2	Calcite		Sp-Ga-Py ore	−4.4	−10.0	19.6	
Tian-3	Calcite		Calcite vein in wall rock	−1.9	−10.5	20.2	
Tian-4	Dolostone		Barren wall rock	−0.7	−11.0	18.6	
Tian-5	Dolostone		Immediate wall rock	−2.3	−10.0	20.6	
Tian-6	Dolostone		Immediate wall rock	−2.5	−10.2	20.4	
YCP2-A	Dolostone	26.8008, 103.7069	Ore-hosting wall rock	0.8	−9.6	21.0	This paper
YCP3-1K	Dolostone		Ore-hosting wall rock	−0.3	−9.7	17.0	
YCP3-5K	limestone		Ore-hosting wall rock	−2.3	−14.4	18.5	
HE11	Dolostone		Ore-hosting wall rock	0.9	−11.2	19.3	Hu, 1999
HE02	Dolostone		Ore-hosting wall rock	0.1	−8.0	22.6	
HE17	Dolostone		Ore-hosting wall rock	0.9	−9.6	21.0	
HE01	limestone		Ore-hosting wall rock	−1.2	−8.0	22.6	
HE12	limestone		Ore-hosting wall rock	−1.1	−10.5	20.1	
HE16	limestone		Ore-hosting wall rock	−0.4	−8.2	22.5	
HE18	limestone		Ore-hosting wall rock	−1.5	−9.2	21.3	

Note: Sp-sphalerite, Ga-galena, Py-pyrite. Analytical uncertainty is 2σ.

(2σ) and $^{206}Pb/^{204}Pb = 16.937 \pm 0.002$ (2σ), in agreement with the reference value (Belshaw et al., 1998).

Chemical separation of Rb and Sr from matrix elements, and mass spectrometric measurement were accomplished at the Institute of Geology and Geophysics, Chinese Academy of Sciences. A detailed analytical procedure for Rb–Sr isotope analyses is available in Li et al. (2005). Spec-Sr exchange resin of special efficiency were used for the separation and purification of Rb and Sr. The whole procedural blank of both Rb and Sr was about 6 pg. Isotopic compositions were measured by the Isoprobe-T Thermal Ionization Mass Spectrometer. An $^{88}Sr/^{86}Sr$ ratio of 8.37521 was used to calibrate mass fractionation of Sr isotope. The average $^{87}Sr/^{86}Sr$ ratio of NBS 987 was 0.710242 ± 5 (2σ, n = 12). The uncertainties (2σ) are 2% for $^{87}Rb/^{86}Sr$ ratios and 0.005% for Sr isotope compositions.

5. Analytical results

5.1. Sulfur isotope compositions

S isotope compositions of pyrite, sphalerite and galena separates from the primary ores of the Tianqiao Pb–Zn deposit, together with previously published data (Gu, 2007; Jin, 2008; Zhou et al., 2010a) are listed in Table 2 and shown in a histogram (Fig. 6A). Galena, sphalerite and pyrite are all enriched in heavy sulfur isotope with $\delta^{34}S_{CDT}$ values ranging from +8.4 to +14.4‰ with an average of +11.7‰ (Table 2; Fig. 6A). Pyrite, sphalerite and galena separates have slightly different $\delta^{34}S$ values, ranging from +12.8 to +14.4‰, +10.9 to +14.2‰ and +8.4 to +12.6‰, respectively. In the paragenetic mineral assemblage, pyrite has the highest $\delta^{34}S$ value, whereas galena has the lowest (Table 2).

5.2. Carbon and oxygen isotope compositions

New and previously published C and O isotope analyses of the Tianqiao Pb–Zn deposit are listed in Table 3. Hydrothermal calcite separates have relatively uniform C and O isotope compositions with $\delta^{13}C_{PDB}$ ranging from −5.3 to −3.4‰ and $\delta^{18}O_{SMOW}$ ranging from +14.9 to +19.6‰. C and O isotope compositions of hydrothermal calcite are obviously different from barren and ore-hosting wall rocks. Barren, ore-hosting and calcite-bearing wall rocks have similar C and O isotope compositions, with $\delta^{13}C_{PDB}$ ranging from −2.3 to +0.9‰ and $\delta^{18}O_{SMOW}$ from +17.0 to +23.6‰, higher than hydrothermal calcite and near to the field of marine carbonate (Fig. 7A). Ore-hosting wall rocks have $\delta^{13}C_{PDB}$ ranging from −3.0 to −2.3‰ and $\delta^{18}O_{SMOW}$ ranging from +20.4 to +20.7‰, higher than hydrothermal calcite, but lower than barren wall rocks, suggesting modification of C and O isotope compositions in the ore-hosting wall rocks by ore-forming fluids.

5.3. Lead isotope compositions

Pb isotope compositions of this deposit and the Huize Pb–Zn deposit, Sinian to Permian carbonate rocks, older basement rocks and Permian Emeishan flood basalts are listed in Tables 4 and 5, respectively. Sulfide samples have relatively homogeneous and characteristically low radiogenic Pb isotope compositions with $^{206}Pb/^{204}Pb$ ranging from 18.378 to 18.601, $^{207}Pb/^{204}Pb$ ranging from 15.519 to 15.811 and $^{208}Pb/^{204}Pb$ ranging from 38.666 to 39.571. Sphalerite separates from different stages have similar Pb isotope compositions (Fig. 8). In the Pb isotope triangle plot, all samples from the Tianqiao deposit are plotted in the Th–Pb field with a few samples along the boundary of the Th–Pb and U–Pb fields (Fig. 9).

Table 4
Pb isotope compositions of the Tianqiao Pb–Zn deposit.

Sample no.	Geographic locality	Mineral	$^{206}Pb/^{204}Pb$	$^{207}Pb/^{204}Pb$	$^{208}Pb/^{204}Pb$	Source
TQ-19	27.0622,	Pyrite	18.526	15.731	38.983	This paper
TQ-24-2	104.5647	Galena	18.521	15.735	38.962	Zhou et al. (2010b)
TQ-24-3		B-Sphalerite	18.481	15.708	38.875	
TQ-24-4		Y-Sphalerite	18.527	15.725	38.929	
TQ-24-5		L-Sphalerite	18.517	15.724	38.930	
TQ-25-1		Galena	18.544	15.763	39.057	
TQ-25-2		L-Sphalerite	18.490	15.713	38.888	This paper
TQ-52		Galena	18.537	15.760	39.040	
TQ-54-1		Galena	18.521	15.726	38.942	
TQ-54-2		Y-Sphalerite	18.504	15.714	38.888	
TQ-60		Pyrite	18.506	15.713	38.901	
Tain-1	27.0585,	Galena	18.538	15.761	39.051	Wang (1993)
Tian-2	104.5709	Galena	18.560	15.772	39.152	
Ty-5		Galena	18.508	15.706	38.934	Zheng (1994)
Ty-7		Galena	18.601	15.782	39.571	
Ty-10		Galena	18.504	15.704	38.872	
HTQ-T1Pb		Galena	18.576	15.804	39.191	Zhang et al. (1998)
HTQ-T2Pb		Galena	18.582	15.811	39.341	
HTQ-T3Pb		Galena	18.539	15.711	39.116	
HTQ-T4Pb		Galena	18.565	15.790	39.115	
HTQ-T5Pb		Galena	18.564	15.776	39.140	
HTQ-T6Pb		Galena	18.517	15.726	39.005	
Jn01	27.0622,	Galena	18.598	15.635	39.112	Liu and Lin (1999)
Jn02	104.5647	Galena	18.438	15.519	38.773	
Pb-37		Galena	18.507	15.701	39.100	
78-01		Galena	18.395	15.632	38.793	
TzPb4		Galena	18.492	15.718	38.934	
TzPb5		Galena	18.454	15.669	38.826	
TzPb6		Galena	18.411	15.673	38.799	
TzPb8		Galena	18.378	15.681	38.666	
TzPb11		Galena	18.446	15.677	38.734	
TzPb12		Galena	18.417	15.677	38.753	
TzPb13		Galena	18.428	15.689	38.792	

Note: Sample no. TQ-24-2, TQ-24-3, TQ-24-4, and TQ-24-5 are selected from the same as sample, TQ-25-1 and TQ-25-2 are selected from the same as sample, and TQ-54-1 and TQ-54-2 are selected from the same as sample. B-Sphalerite is brown sphalerite, Y-Sphalerite is brownish-yellow sphalerite and L-Sphalerite is light yellow sphalerite. Analytical uncertainty is 2σ.

Table 5
Statistical results of the Pb isotope compositions of the Tianqiao Pb–Zn deposit, Sinian to Permian carbonate rocks, Precambrian basement rocks and Permian Emeishan flood basalts.

Statistical object		Number of samples	$(^{206}Pb/^{204}Pb)_{200\ Ma}$		$(^{207}Pb/^{204}Pb)_{200\ Ma}$		$(^{208}Pb/^{204}Pb)_{200\ Ma}$	
			Range	Mean	Range	Mean	Range	Mean
Tianqiao Pb–Zn deposit		33	18.378–18.601	18.506	15.519–15.811	15.716	38.666–39.571	38.975
Mineral	Galena	26	18.378–18.601	18.505	15.519–15.811	15.715	38.666–39.571	38.991
	Sphalerite	5	18.506–18.526	18.516	15.713–15.731	15.722	38.901–38.983	38.942
	Pyrite	2	18.481–18.527	18.504	15.708–15.725	15.717	38.875–38.930	38.902
Huize Pb–Zn deposit		95	18.251–18.530	18.465	15.439–15.855	15.717	38.487–39.433	38.894
Mineral or Ore	Galena	25	18.251–18.530	18.453	15.672–15.855	15.712	38.487–39.433	38.875
	Sphalerite	24	18.339–18.500	18.454	15.663–15.754	15.716	38.719–38.996	38.881
	Pyrite	27	18.393–18.514	18.478	15.664–15.751	15.725	38.729–39.009	38.906
	Ore	19	18.437–18.494	18.474	15.437–15.744	15.713	38.868–38.975	38.919
Lower Permian Qixia-Maokou Fm., Limestone		12	18.189–18.759	18.474	15.609–16.522	16.066	38.493–38.542	38.518
Upper Carboniferous Huanglong Fm., Limestone		12	18.136–18.167	18.152	15.656–16.675	15.666	38.204–38.236	38.220
Lower Carboniferous Baizuo Fm., Dolostone		28	18.120–18.673	18.380	15.500–16.091	15.743	38.235–39.685	38.777
Lower Carboniferous Dapu Fm., Dolostone		15	18.397–18.828	18.596	15.537–16.499	15.804	38.463–39.245	38.885
Upper Devonian Zaige Fm., Limestone		13	18.245–18.842	18.542	15.681–16.457	16.012	38.715–39.562	38.998
Upper Sinian Dengying Fm., Dolostone		20	18.198–18.517	18.360	15.699–15.987	15.818	38.547–39.271	38.909
Basement Kunyang Group		27	17.781–20.993	18.789	15.582–15.985	15.686	37.178–40.483	38.427
Basement Huili Group		16	18.094–18.615	18.287	15.630–15.827	15.708	38.274–38.932	38.585
Permian Emeishan flood basalts		56	18.175–19.019	18.541	15.528–15.662	15.574	38.380–39.928	38.983

Note: Pb isotope compositions of the Huize Pb–Zn deposit are taken from Han et al. (2007a), Li et al. (2007b) and Zhou et al. (2001). Sources of other data are taken from Han et al. (2007a, 2012), Hu (1999), Liu and Lin (1999), Wang et al. (2000, 2003, 2010), Yan et al. (2007), Zheng and Wang (1991), Zhou et al. (2001), and this work. $(^{206}Pb/^{204}Pb)_t = (^{206}Pb/^{204}Pb)_p - \mu(e^{\lambda t} - 1)$, $(^{207}Pb/^{204}Pb)_t = (^{207}Pb/^{204}Pb)_p - \mu/137.88(e^{\lambda' t} - 1)$, $(^{208}Pb/^{204}Pb)_t = (^{208}Pb/^{204}Pb)_p - \omega(e^{\lambda'' t} - 1)$, $\lambda = 1.55125\times10^{-10}t^{-1}$, $\lambda' = 9.8485\times10^{-10}t^{-1}$, $\lambda'' = 0.49475\times10^{-10}t^{-1}$, $t = 200$Ma.

5.4. Rb–Sr isotope compositions and isochron age

Sphalerite and pyrite separates are analyzed for Rb–Sr isotope (Table 6). These separates have $^{87}Rb/^{86}Sr$ ratios ranging from 0.0296 to 1.5640. $^{87}Sr/^{86}Sr$ ratios of sphalerite and pyrite are relatively homogeneous and range from 0.7125 to 0.7167. The analyses yield an Rb–Sr isochron age of 191.9 ± 6.9 Ma, with an initial $^{87}Sr/^{86}Sr$ ratio of 0.7124 and MSWD of 0.39 (Fig. 10A).

6. Discussion

6.1. Possible sources of sulfur

Primary ores from the Tianqiao Pb–Zn deposit are composed chiefly of galena, sphalerite and pyrite. The lack of sulfate minerals in the ores suggests that $\delta^{34}S$ value of sulfide can basically represent the total S isotope composition of the hydrothermal fluid, i.e. $\delta^{34}S_{\sum S} \approx \delta^{34}S_{sulfide}$ (Ohmoto, 1972). All ore minerals, including galena, sphalerite and pyrite, have relatively enriched heavy S isotope with $\delta^{34}S$ values in the range of +11 to +14‰ (Fig. 6A and Table 2), significantly different from that of mantle-derived S (~0‰: Chaussidon et al., 1989). On the other hand, sedimentary rocks in the mining area contain sulfate minerals that have high $\delta^{34}S$ values, such as gypsum (~+15‰; Liu and Lin, 1999) and barite (+22 to +28‰; Han et al., 2007a; Jin, 2008). Therefore, evaporites of Devonian to Carboniferous sedimentary rocks may have provided sulfur for ore-forming fluids.

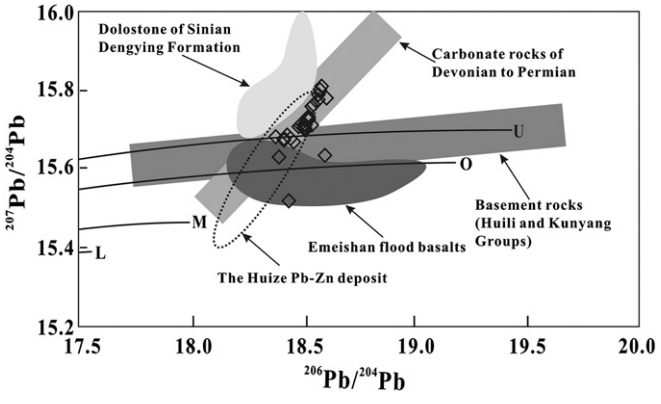

Fig. 8. Plots of $^{207}Pb/^{204}Pb$ vs. $^{206}Pb/^{204}Pb$ for the Tianqiao Pb–Zn deposit. Trends for the upper crust (U), orogen (O), mantle (M) and lower crust (L) are taken from Zartman and Doe (1981). Pb isotope compositions of the Huize Pb–Zn deposit are taken from Han et al. (2007a), Li et al. (2007b) and Zhou et al. (2001). Sources of other data are taken from Han et al. (2007a), Hu (1999), Liu and Lin (1999), Yan et al. (2007), Zhou et al. (2001) and this work.

Possible mechanism for reduced sulfur from sulfate includes bacterial sulfate reduction (BSR) and thermo-chemistry sulfate reduction (TSR) (e.g. Basuki et al., 2008; Seal, 2006). These processes are temperature-dependent. BSR occurs under relatively low temperatures (below 120 °C; Dixon and Davidson, 1996; Jorgenson et al., 1992; Machel, 1989). TSR takes place under relatively high temperatures (above 175 °C; Basuki et al., 2008; Ohmoto et al., 1990). S isotope fractionation has reached equilibrium in hydrothermal fluids for the Tianqiao deposit, similar to the Huize Pb–Zn deposit (Fig. 6B; Han et al., 2007a), and so mineralization temperature can be calculated by using sulfur isotope balance fractionation equation with $\Delta^{34}S_{pyrite-sphalerite}$ values (Czamanske and Rye, 1974). The calculated equilibrium temperatures range from 170 °C to 300 °C, similar to the homogenization temperature of fluid inclusions in calcite (150 °C to 240 °C; Jin, 2008). Previous studies have confirmed that the reaction $SO_4^{2-} + CH_4 = H_2S + CO_3^{2-} + H_2O$ can take place at 140 °C (Worden et al., 1995). Therefore, TSR was the main mechanism that transferred SO_4^{2-} from sulfate into H_2S in hydrothermal solutions.

6.2. Origin of CO_2 in hydrothermal fluids

In the diagram of $\delta^{13}C_{PDB}$ vs. $\delta^{18}O_{SMOW}$ (Fig. 7A), all samples are plotted in the field of mantle, marine carbonate and sedimentary organic matter, and near to marine carbonate rocks. If CO_2 in hydrothermal fluids was derived from mantle, precipitated hydrothermal calcite would show constant $\delta^{13}C$ with high $\delta^{18}O$ values (Demény et al., 1998). Similarly, if CO_2 was originated from marine carbonate rocks, precipitated hydrothermal calcite would display constant $\delta^{13}C_{PDB}$ with low $\delta^{18}O_{SMOW}$ values (Demény and Harangi, 1996). Therefore, the approximately negative correlation between $\delta^{13}C_{PDB}$ and $\delta^{18}O_{SMOW}$ values (Fig. 7B) indicates that the CO_2 of hydrothermal fluids were derived neither from mantle or marine carbonate rocks, nor from sedimentary organic matters. Because organic matters can act as reducing agent in TSR process (e.g. Ottaway et al., 1994;

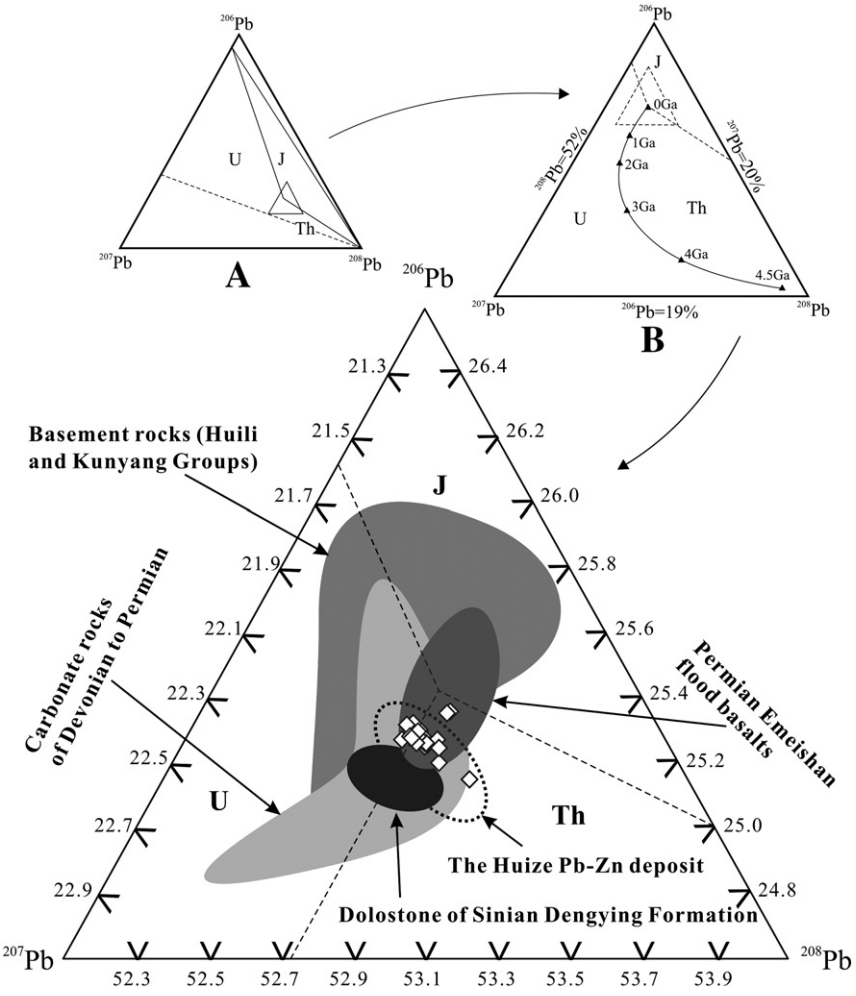

Fig. 9. Plots of $^{206}Pb/^{204}Pb$–$^{207}Pb/^{204}Pb$–$^{208}Pb/^{204}Pb$ for the Tianqiao Pb–Zn deposit. Pb isotope compositions of the Huize Pb–Zn deposit are taken from Han et al. (2007a), Li et al. (2007b) and Zhou et al. (2001). Sources of other data are taken from Han et al. (2007a), Hu (1999), Liu and Lin (1999), Yan et al. (2007), Zhou et al. (2001), and this work.

Worden et al., 1995), so the organic matter is also an important contributor of CO_2. Therefore, a mixture of ternary members is a possible origin of CO_2. There are ^{18}O-depleted Permian Emeishan flood basalts, ^{18}O-enriched Devonian to Carboniferous carbonate rocks and ^{13}C-depleted organic matters in Devonian to Permian sedimentary rocks (Fig. 7A).

6.3. Possible sources of ore-forming metals

Earlier studies suggested that metals of the Tianqiao Pb–Zn deposit were sources from host Devonian to Carboniferous carbonate rocks (e.g. Mao, 2000; Mao et al., 1998, 2001; Wang, 1994; Wang et al., 1996; Zheng, 1994). On the other hand, Li et al. (1999) suggested that Sinian to Carboniferous sedimentary rocks were important sources of metals. However, other researchers considered that metals were derived from Precambrian basement rocks (e.g. Hu, 1999; Jin, 2008; Zhou et al., 2001). The coarse-grained recrystallized dolostone implies that the metals in these host carbonate rocks were remobilized, so we conclude that the Devonian to Permian carbonate rocks were an important source of metals. The Emeishan flood basalts have relatively uniform Pb and Zn contents (Huang et al., 2004), somewhat higher than the Devonian to Permian carbonate rocks and the Clarke value, suggesting that the basalts may also have provided partially metals (e.g. Han et al., 2007a; Huang et al., 2003, 2004, 2010; Liu and Lin, 1999).

6.3.1. Constraints of Pb isotope

Sulfide minerals from the Tianqiao Pb–Zn deposit have relatively constant Pb isotopes (Table 4), indicative of derivation of Pb metal in ore-forming fluids from geological bodies with homogeneous Pb

Table 6
Sulfide Rb–Sr isotopes compositions of the Tianqiao Pb–Zn deposit.

Sample no.	Object	$Rb/10^{-6}$	$Sr/10^{-6}$	$^{87}Rb/^{86}Sr$	$^{87}Sr/^{86}Sr$	$(^{87}Sr/^{86}Sr)$ t	2σ
TQ-60	Y-Sphalerite	0.03	2.40	0.0406	0.7126	0.7124	0.0001
TQ-19-1	Pyrite	0.02	2.20	0.0296	0.7125	0.7124	0.0001
TQ-19-2	Y-Sphalerite	0.01	0.80	0.0324	0.7126	0.7125	0.0001
TQ-26-0	Y-Sphalerite	0.60	1.10	1.5640	0.7167	0.7123	0.0001
TQ-26-1	Y-Sphalerite	0.47	0.90	1.0101	0.7152	0.7123	0.0001

Note: TQ-19-1 and TQ-19-2 take from sample TQ-19, TQ-26-0 and TQ-26-1 take from sample TQ-26. Y-Sphalerite is brownish yellow sphalerite. $(^{87}Sr/^{86}Sr)_t = {}^{87}Sr/^{86}Sr - {}^{87}Sr/^{87}Rb(e^{\lambda t}-1)$, $\lambda_{Rb} = 1.41\times10^{-11}\ t^{-1}$, $t = 200$Ma.

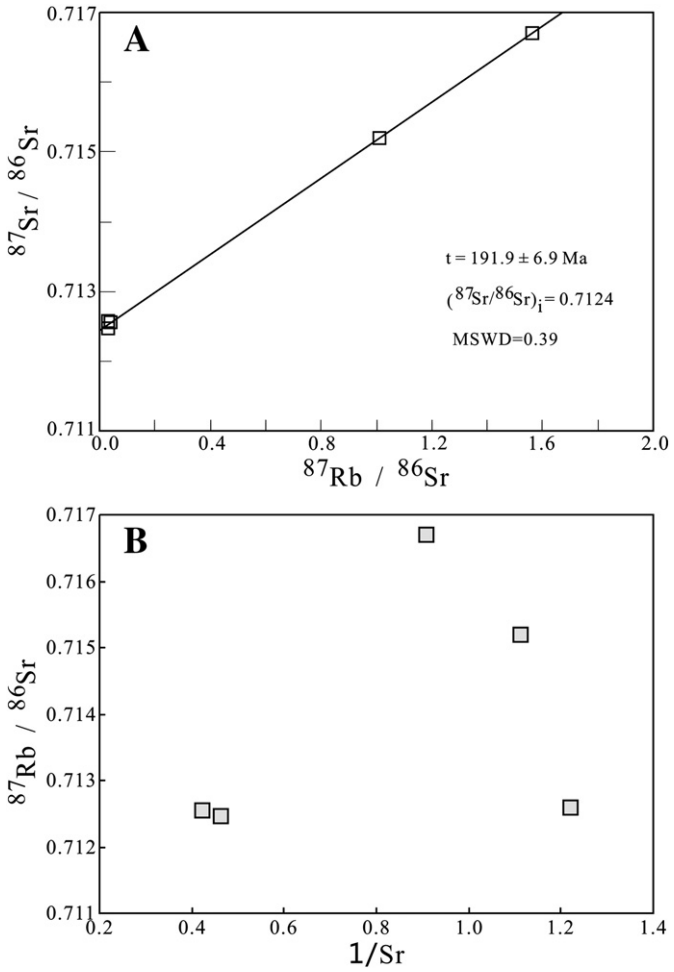

Fig. 10. Plot of sulfide Rb–Sr isochron for the Tianqiao Pb–Zn deposit (A) and plot of sulfide $^{87}Sr/^{86}Sr$ vs. 1/Sr for the Tianqiao Pb–Zn deposit (B).

isotopes, or with variable Pb isotopes, but have been homogenized before the Pb–Zn mineralization. We note that the older basement rocks, the younger cover Sinian to Permian sedimentary rocks and Permian Emeishan flood basalts have variable Pb isotopes (Table 5). Pb isotopes of sulfide minerals from the Tianqiao deposit are similar to those of basalts, sedimentary rocks and basement rocks (Figs. 8 and 9; Tables 4 and 5). It demonstrates that Pb metal may have multiple-sources, presumably including basalts, sedimentary rocks and basement rocks in the SYG province. Therefore, we believe that the Pb isotopes of the Tianqiao Pb–Zn deposit reflect homogenization of Pb isotopes in hydrothermal fluids before the Pb–Zn mineralization.

6.3.2. Constraints of Sr isotopes

Based on the age of Pb–Zn mineralization in the SYG province (about ~200 Ma), we calculate the initial Sr isotope compositions of sulfides and whole-rocks. Sulfide separates from the Tianqiao Pb–Zn deposit have initial $^{87}Sr/^{86}Sr$ ratios ranging from 0.7123 to 0.7125, higher than the upper mantle (0.704 ± 0.002; Faure, 1977) and Permian Emeishan flood basalts (0.7039 to 0.7078; Huang et al., 2004). Sinian to Permian sedimentary rocks have $(^{87}Sr/^{86}Sr)_t$ (t = 200Ma) ratios ranging from 0.7073 to 0.7111 (Table 7, including data from Deng et al., 2000; Hu, 1999), also lower than sulfides (Fig. 11). The Precambrian Dongchuan and Huili Groups are widely distributed in the western Yangtze Block (e.g. Sun et al., 2009; Yan et al., 2003; Zhang et al., 1988; Zhao et al., 2010). They have $(^{87}Sr/^{86}Sr)_t$ (t = 200 Ma) ratios ranging from 0.7243 to 0.7288 (Table 7; Chen and Ran, 1992; Li and Qin, 1988), higher than sulfides (Fig. 11). Therefore, both the older basement rocks with high $^{87}Sr/^{86}Sr$ ratios and the younger sedimentary rocks and basalts with low $^{87}Sr/^{86}Sr$ ratios may have provided ore strontium for hydrothermal fluids.

6.4. A possible genetic model for the ore deposition

6.4.1. Timing of the mineralization in the SYG province

Previous studies demonstrate that the sulfide Rb–Sr isotopic dating is feasible for certain sulfide minerals (e.g. Christensen and Halliday, 1995; Christensen et al., 1995; Nakai et al., 1993). For example, sphalerite may host Rb in its lattice preferentially than Sr, and thus has high $^{87}Rb/^{86}Sr$ ratios, making the mineral suitable for precise radiogenic isotope dating. This method has been applied to hydrothermal deposits (e.g. Christensen and Halliday, 1995; Christensen et al., 1995; Nakai et al., 1993; Yin et al., 2009). A modified single grain Rb–Sr isotopic dating with high precise TIMS and ultra-low procedural blank is also used for pyrite (e.g. Han et al., 2007b; Li et al., 2008) and sphalerite (e.g. Lin et al., 2010; Zhang et al., 2008).

The Rb–Sr isotopic age of 191.9 ± 6.9 Ma of sulfides from the Tianqiao deposit is considered to be reliable. The fact that 1/Sr values do not co-vary with $^{87}Sr/^{86}Sr$ ratios of samples (Fig. 10B) indicate that the isochron age is not a pseudoisochron and has isochronal meaning (e.g. Lin et al., 2010; Nakai et al., 1993; Yin et al., 2009; Zhang et al., 2008). Therefore, this age is interpreted to reflect the timing of the Pb–Zn mineralization. Hydrothermal calcite of the Huize Pb–Zn deposit has a Sm–Nd isotopic age of 222 ± 14 Ma (Li et al., 2007a). Sphalerite of the Paoma Pb–Zn deposit has an Rb–Sr isotopic age of 200.1 ± 4.0 Ma (Lin et al., 2010). Our Rb–Sr isotopic age is broadly similar to these early reported ages. Therefore, we consider that

Table 7
Sr isotope compositions of sulfide, Sinaian to Permian sedimentary rocks, Permian Emeishan flood basalts and upper mantle.

Object	Geographic locality	Num.	$(^{87}Sr/^{86}Sr)_t$ (t = 200Ma)		Source
			Range	Mean	
Sphalerite from the Tianqiao deposit	27.0622, 104.5647	5	0.7123–0.7125	0.7124	This paper
Lower Permian Qixia Fm., Limestone	26.6351, 103.7267	3	0.7073–0.7089	0.7075	This paper and Deng et al. (2000)
Upper Carboniferous Maping Fm., Limestone	26.6426, 103.7247	2	0.7099–0.7100	0.7100	This paper
Lower Carboniferous Baizuo Fm., Dolostone	26.6402, 103.7252	5	0.7087–0.7101	0.7094	This paper and Hu (1999)
Upper Devonian Zaige Fm., Limestone	26.6405, 103.6951	2	0.7084–0.7088	0.7086	This paper
Middle Devonian Qujing Fm., Dolostone	27.0689, 103.3539	1	0.7101	0.7101	Deng et al. (2000)
Middle Devonian Haikou Fm., Sandstone	26.6295, 103.6667	1	0.7111	0.7111	This paper
Upper Sinian Dengying Fm., Dolostone	26.6316, 103.6985	2	0.7083–0.7096	0.7089	
Permian Emeishan flood basalts	26.6465, 103.6911	85	0.7039–0.7078	0.7058	Cong (1988), Li and Qin (1988), Chen and Ran (1992), and Huang et al. (2004)
Kunyang and Huili Groups		5	0.7243–0.7288	0.7268	
Upper mantle			0.704 ± 0.002	0.704	Faure (1977)

Note: $(^{87}Sr/^{86}Sr)_t = {}^{87}Sr/^{86}Sr - {}^{87}Sr/^{87}Rb\ (e^{\lambda t} - 1)$, $\lambda_{Rb} = 1.41 \times 10^{-11}\ t^{-1}$, t = 200Ma. Analytical uncertainty is 2σ.

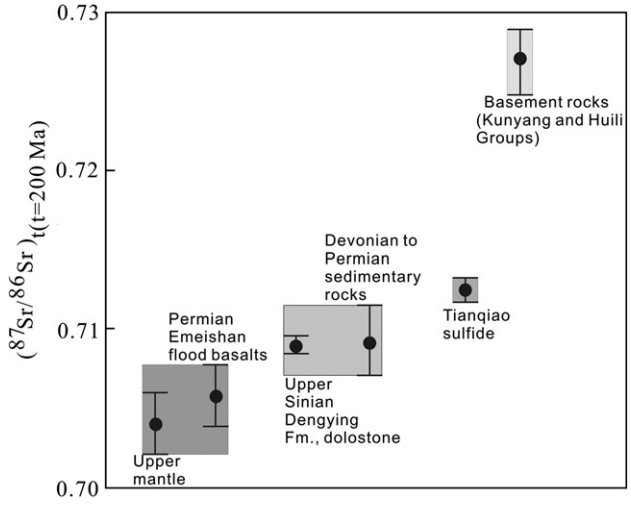

Fig. 11. Comparison of $(^{87}Sr/^{86}Sr)_t$ (t = 200Ma) ratios among Tianqiao Pb–Zn deposits, sedimentary rocks, basement rocks, Emeishan basalts and upper mantle. Sources of whole rocks strontium are taken from Chen and Ran (1992), Cong (1988), Deng et al. (2000), Li and Qin (1988), Han et al. (2007a), Hu (1999), Huang et al. (2004), Zhou et al. (2001) and this work.

these deposits formed simultaneously and that the main mineralization of the SYG province occurred at ~200 Ma.

6.4.2. Geodynamic setting and possible related thermal event

All the Pb–Zn deposits in the SYG province have many common features, suggesting that they may belong to the same type of deposits (Han et al., 2007a, 2012; Huang et al., 2004, 2010; Jin, 2008; Li et al., 2007a; Liu and Lin, 1999; Wang et al., 2000, 2003, 2010; Yin et al., 2009; Zheng and Wang, 1991; Zhou et al., 2001, 2010a, 2010b, 2011). Because ore bodies are hosted in carbonate rocks, these deposits are thought to be a typical type of MVT (e.g. Wang et al., 2000, 2003, 2010; Zheng and Wang, 1991; Zhou et al., 2001). However, many aspects of these deposits are different from typical MVT deposits (Table 8). For example, they have homogeneous but non-radiogenic Pb isotope compositions (e.g. Han et al., 2007a; Li et al., 2007b) and much higher Pb and Zn grades (6.92–20.51 wt.% Pb + Zn; Han et al., 2007a, 2012) than MVT deposits (less than 10 wt.% Pb + Zn). Typical MVT deposits are not linked with known igneous activities and associated with the extensional basin formation (e.g. Leach and Sangster, 1993). The thrust faults indicative of a compression geodynamic setting (Figs. 2 and 3) in the SYG province are also different from the extensional geodynamic setting of typical MVT. Pb–Zn deposits in the SYG province are much younger than Permian Emeishan flood basalts (~260 Ma: Zhou et al., 2002a) and are not thought to be related to the Emeishan magmatism. However, C–O–S–Pb–Sr isotopes indicate contribution of Permian Emeishan flood basalts to Pb–Zn mineralization and there is close association of the flood basalts and deposits (Fig. 1B). In addition, within the SYG province, mantle-derived alkaline plutons range in ages from 204 to 225 Ma (e.g. Liu et al., 2004). Tectonically, in the late Triassic–early Jurassic (~200 Ma), the Yangtze Block was collided with adjacent blocks associated the closure of the Tethys Ocean (e.g. Reid et al., 2007; Zhang et al., 2006). This event is known as the Indosinian Orogeny and has led to the deformation through thrust fault–fold structure (Han et al., 2012) in the Tianqiao Pb–Zn ore field (Figs. 2 and 3). Therefore, the Pb–Zn deposits in the SYG province are considered a unique type of Pb–Zn deposits, namely SYG type (e.g. Han et al., 2007a, 2012; Huang et al., 2003, 2010), different from typical MVT deposits (e.g. Leach and Sangster, 1993; Leach et al., 2010).

6.4.3. An integrated model and mineralization process

We propose a possible genetic model for the ore deposition. The ~260 Ma mantle plume activity produced the Emeishan flood basalts in the western Yangtze Block above the Lower Permian strata (Fig. 1A and B). The upwelling mantle plume eventually resulted in the thinning of the crust and deposition of Triassic sedimentary rocks above

Table 8
Comparison of the Tianqiao and Huize Pb–Zn deposits with typical MVT worldwide.

Characteristics	The Tianqiao Pb–Zn deposit	The Huize Pb–Zn deposit	MVT Pb–Zn deposits
Grade	Pb + Zn: 6.92–20.51 wt.%, Zn/(Zn + Pb): 0.75 ±	Pb + Zn: average 35 wt.%, Zn/(Zn + Pb): 0.9 ±	Pb + Zn: less than 10 wt.%, Zn/(Zn + Pb): 0.8 ±
Tonnage	Pb + Zn reserves are more than 0.2 Mt	Pb + Zn reserves of single ore-body close to 1 Mt	Pb + Zn reserves of single ore-body less than 1 Mt
Acreage	Area of SYG metallogenic province about 170,000 km^2	Area of SYG metallogenic province about 170,000 km^2	Hundreds square kilometers
Host rocks	Devonian and Carboniferous coarse-crystalline dolomite	Carboniferous coarse-crystalline dolomite	Carboniferous, Devonian, Ordovician and Cambrian carbonate rocks
Depth of mineralization	More than 400 m	More than 2000 m	No more than 1500 m
Tectonic setting	Western margin of the Yangtze Block, controlled by the NW thrust fault	Western margin of the Yangtze Block, controlled by Qilingchang thrust fault	Generally related with extensional basin
Relation with magmatic activity	Permian Emeishan flood basalts and diabase	Permian Emeishan flood basalts	Generally no genetic connection with magmatic activity in time and space
Ore-controlled factors	Controlled by structure and lithology	Controlled by structure and lithology	Mainly controlled by structure and lithology
Age	About 192 Ma	About 225 Ma	From Proterozoic to Cretaceous
Ore texture and structure	Mainly exhibiting massive structures and fine-medium-coarse grained textures	Mainly exhibiting massive structures and fine-medium-coarse grained textures	Exhibiting disseminated, fine granular, branched, colloidal and massive structures and colloidal, skeleton coarse-crystalline textures
Mineral compositions	Sphalerite, galena, pyrite, calcite and dolomite	Sphalerite, galena, pyrite and calcite	Sphalerite, galena, pyrite, chalcopyrite, barite, fluorite, calcite and dolomite, etc.
Fluid inclusions	10 wt.% salinity; Cl^-–Na^+–Ca^{2+}–F^-–SO_4^{2-}; 150–240 °C	10 wt.% salinity; Cl^-–Na^+–Ca^{2+}–F^-–SO_4^{2-}; 150–250 °C	10–30 wt.% salinity; Cl^-–Na^+–Ca^{2+}–K^+–Mg^{2+}; 50–200 °C
Associated metals	Ag, Ge, Ga, Cd and In	Ag, Ge, Ga, Cd and In	Most deposits with Ag, some with Cu, Co, Ni
S isotopes	+8–+15‰	+11–+17‰	+10–+25‰
Pb isotopes	Homogenization Pb isotope composition and normal Pb isotopes	Homogenization Pb isotope composition and normal Pb isotopes	Complicated Pb isotope composition and regional zonation

Note: The Tianqiao Pb–Zn deposit is taken from Jin (2008), Zhou et al. (2010a, 2010b, 2011) and this paper. The Huize Pb–Zn deposit is taken from Han et al. (2007a, 2012), Huang et al. (2004, 2010) and Zhou et al. (2001). The MVT Pb–Zn deposits are taken from Anderson (1975), Anderson and MacQueen (1982), Basuki and Spooner (2002), Bradley and Leach (2003), Gibbins (1983), Leach and Sangster (1993, 1996), Leach et al. (2001, 2006, 2010) and Sangster (1983, 1996).

the Permian Emeishan flood basalts and sedimentary rocks. Thermal activity related to the Indosinian Orogeny resulted in hydrothermal fluids and mineralization of ore-forming metals from Devonian to Permian sedimentary rocks. Extensive fluid migration and circulation resulted in reduction of reduced sulfur from gypsum and barite in Cambrian to Permian sedimentary rocks by TSR. In addition to the Paleozoic sedimentary rocks, the Pb–Zn enriched Precambrian rocks may have provided the Pb–Sr metals for the hydrothermal fluids. Circulation of hydrothermal fluids underneath the Emeishan flood basalts made the fluids homogenized isotopically, whereas the basalts acted as an impermeable layer. At about 200 Ma, driven by tectonic and thermal dynamics, the resulting hydrothermal fluids were enriched in metals when migrated upward along regional faults, such as the Weining–Shuicheng and Yadu–Mangdong faults (Fig. 1C), and incorporated reduced sulfur-bearing solutions, leading to the precipitation of the Pb–Zn ores along fracture zones and inter-formational boundaries (Fig. 2).

7. Conclusions

1) The Tianqiao Pb–Zn deposit is hosted in Devonian to Carboniferous carbonate rocks and its ore bodies are structurally controlled by a thrust fault and anticline.
2) Evaporites of the host strata provided reduced sulfur for the hydrothermal fluids by TSR, whereas CO_2 had mixed sources of basalts, carbonate rocks and organic matters.
3) Sedimentary rocks, basalts and basement rocks provided ore-forming metals, and Pb–Sr isotopes of metal-bearing hydrothermal fluids were homogenized before Pb–Zn mineralization.
4) Timing of Pb–Zn mineralization in the SYG province is ~200 Ma, younger than the Permian Emeishan Large Igneous Province, but the flood basalts probably acted as an impermeable layer for ore deposition from the hydrothermal fluids.

Acknowledgment

This research was financially supported by the National Natural Science Foundation of China (Nos. 41102055 and 41102053), the National Basic Research Program of China (973 Program) (No. 2007CB411402) and the Knowledge Innovation Project of the Chinese Academy of Sciences (Nos. KZCX2-YW-Q04-05 and KZCX2-YW-111-03). Thanks are given to Dr. Jianfeng Gao and Prof. Lin Ye for useful discussion. Comments and suggestions from Prof. Graham Carr, David Huston, Franco Pirajno, Runsheng Han and anonymous reviewers greatly improved the quality of the paper.

References

Anderson, G.M., 1975. Precipitation of Mississippi Valley-type ores. Econ. Geol. 70, 937–942.
Anderson, G.M., MacQueen, R.W., 1982. Ore deposit models — 6. Mississippi Valley-type lead–zinc deposits. Geosci. Can. 9, 108–117.
Basuki, N.I., Spooner, E.T.C., 2002. A review of fluid inclusion temperatures and salinities in Mississippi Valley-type Zn–Pb deposits: identifying thresholds for metal transport. Explor. Min. Geol. 11, 1–17.
Basuki, N.I., Taylor, B.E., Spooner, E.T.C., 2008. Sulfur isotope evidence for thermochemical reduction of dissolved sulfate in Mississippi valley type zinc–lead mineralization, Bongara area, northern Peru. Econ. Geol. 103, 183–799.
Belshaw, N.S., Freedman, P.A., O'Nions, R.K., Frank, M., Guo, Y., 1998. A new variable dispersion double-focusing plasma mass spectrometer with performance illustrated for Pb isotopes. Int. J. Mass Spectrom. 181, 51–58.
Bradley, D.C., Leach, D.L., 2003. Tectonic controls of Mississippi Valley-type lead–zinc mineralization in orogenic forelands. Miner. Deposita 38, 652–667.
Carr, G.R., Dean, J.A., Suppel, D.W., Heithersay, P.S., 1995. Precise lead isotope fingerprinting of hydrothermal activity associated with Ordovician to Carboniferous metallogenic events in the Lachlan fold belt of New South Wales. Econ. Geol. 90, 1467–1505.
Chaussidon, M., Albarède, F., Sheppard, S.M.F., 1989. Sulphur isotope variations in the mantle from ion microprobe analyses of micro-sulphide inclusions. Earth Planet. Sci. Lett. 92, 144–156.
Chen, S.J., 1986. A discussion on the sedimentary origin of Pb–Zn deposits in western Guizhou and northeastern Yunnan. Guizhou Geol. 8, 35–39 (in Chinese with English abstract).
Chen, H.S., Ran, C.Y., 1992. Isotope Geochemistry of Copper Deposit in Kangdian area. Geological Publishing House, Beijing, pp. 1–25 (in Chinese).
Christensen, J.N., Halliday, A.N., 1995. Direct dating of sulfides by Rb–Sr: a critical test using the Polaris Mississippi Valley-type Zn–Pb deposit. Geochim. Cosmochim. Acta 59, 5191–5197.
Christensen, J.N., Halliday, A.N., Vearncombe, J.R., Kesler, S.E., 1995. Testing models of large-scale crustal fluid flow using direct dating of sulfides: Rb–Sr evidence for early dewatering and formation of Mississippi Valley-type deposits, Canning Basin, Australia. Econ. Geol. 90, 877–884.
Chung, S.L., Jahn, B.M., 1995. Plume–lithosphere interaction in generation of the Emeishan flood basalts at the Permian–Triassic boundary. Geology 23, 889–892.
Cong, B.L., 1988. Evolution and Formation of Panxi Rift. Science Press, Beijing, pp. 10–33 (in Chinese).
Cromie, P.W., Gosse, R.R., Zhang, P., Zhu, X., 1996. Exploration for Carbonate-hosted Pb–Zn Deposits, Sichuan, P.R.C. [abs.]: International Geological Congress, 30th, Beijing, China, p. 412 (Abstracts).
Czamanske, G.K., Rye, R.O., 1974. Experimentally determined sulfur isotope fractionations between sphalerite and galena in the temperature range 600 °C to 275 °C. Econ. Geol. 69, 17–25.
Demény, A., Harangi, S.Z., 1996. Stable isotope studies on carbonate formations in alkaline basalt and lamprophyre series: evolution of magmatic fluids and magma-sediment interactions. Lithos 37, 335–349.
Demény, A., Ahijado, A., Casillas, R., Vennemann, T.W., 1998. Crustal contamination and fluid/rock interaction in the carbonatites of Fuerteventura (Canary Islands, Spain): a C, O, H isotope study. Lithos 44, 101–115.
Deng, H.L., Li, C.Y., Tu, G.Z., Zhou, Y.M., Wang, C.W., 2000. Strontium isotope geochemistry of the Lemachang independent silver ore deposit, northeastern Yunnan, China. Sci. China Ser. D Earth Sci. 43, 337–346.
Dixon, G., Davidson, G.J., 1996. Stable isotope evidence for thermochemical sulfate reduction in the Dugald River (Australia) strata-bound shale-hosted zinc–lead deposit. Chem. Geol. 129, 227–246.
Faure, G., 1977. Principles of Isotope Geology. John Wiley & Sons, New York, pp. 28–110.
Friedman, I., O'Neil, J.R., 1977. Compilation of stable isotope fractionation factors of geochemical interest. Data of Geochemistry, U.S. Geological Survey Professional Paper, 440-KK, pp. 1–12.
Gao, S., Yang, J., Zhou, L., Li, M., Hu, Z., Guo, J., Yuan, H., Gong, H., Xiao, G., Wei, J., 2011. Age and growth of the Archean Kongling terrain, South China, with emphasis on 3.3 Ga granitoid gneisses. Am. J. Sci. 311, 153–182.
Gibbins, W.A., 1983. Mississippi Valley-type lead–zinc districts of northern Canada. In: Kisvarsanyi, G., Grant, S.K., Pratt, W.P., Koenig, J.W. (Eds.), International Conference on Mississippi Valley-type lead–zinc deposits: Proceedings Volume Rolla, Missouri, University of Missouri, Rolla, pp. 403–414.
Gu, S.Y., 2007. Study on the sulfur isotope compositions of lead–zinc deposits in northwestern Guizhou Province. J. Guizhou Univ. Technol. 36, 8–13 (in Chinese with English abstract).
Guan, S.P., Li, Z.X., 1999. Lead–sulfur isotope study of carbonate-hosted Pb–Zn deposits at the eastern margin of the Kangdian axis. Geol. Geochem. 27, 45–54 (in Chinese with English abstract).
Haest, M., Schneider, J., Cloquet, C., Latruwe, K., Vanhaecke, F., Muchez, P., 2010. Pb isotopic constraints on the formation of the Dikulushi Cu–Pb–Zn–Ag mineralisation, Kundelungu Plateau (Democratic Republic of Congo). Miner. Deposita 45, 393–410.
Han, R.S., Liu, C.Q., Huang, Z.L., Chen, J., Ma, D.Y., Lei, L., Ma, G.S., 2007a. Geological features and origin of the Huize carbonate-hosted Zn–Pb–(Ag) District, Yunnan, South China. Ore Geol. Rev. 31, 360–383.
Han, Y.G., Li, X.H., Zhang, S.H., Zhang, Y.H., Chen, F.K., 2007b. Single grain Rb–Sr dating of euhedral and cataclastic pyrite from the Qiyugou gold deposit in western Henan, central China. Chin. Sci. Bull. 52, 1820–1826.
Han, R.S., Hu, Y.Z., Wang, X.K., Hou, B.H., Huang, Z.L., Chen, J., Wang, F., Wu, P., Li, B., Wang, H.J., Dong, Y., Lei, L., 2012. Mineralization model of rich Ge–Ag bearing Zn–Pb polymetallic deposit concentrated district in northeastern Yunnan, China. Acta Geol. Sin. 86, 280–294 (in Chinese with English abstract).
Herlec, U., Spangenberg, J.E., Lavrič, J.V., 2010. Sulfur isotope variations from orebody to hand-specimen scale at the Mežica lead–zinc deposit, Slovenia: a predominantly biogenic pattern. Miner. Deposita 45, 531–547.
Hu, Y.G., 1999. Ag occurrence, source of ore-forming metals and mechanism of Yinchangpo Ag–Pb–Zn deposit, Guizhou. Ph.D. Thesis, Institute of Geochemistry, CAS, pp. 10–55 (in Chinese with English abstract).
Hu, R.Z., Zhou, M.F., 2012. Multiple Mesozoic mineralization events in South China—an introduction to the thematic issue. Miner. Deposita 47, 579–588.
Huang, Z.L., Li, W.B., Chen, J., Han, R.S., Liu, C.Q., Xu, C., Guan, T., 2003. Carbon and oxygen isotope constraints on the mantle fluids join the mineralization of the Huize super-large Pb–Zn deposits, Yunnan Province, China. J. Geochem. Explor. 78 (79), 637–642.
Huang, Z.L., Chen, J., Han, R.S., Li, W.B., Liu, C.Q., Zhang, Z.L., Ma, D.Y., Gao, D.R., Yang, H.L., 2004. Geochemistry and Ore-formation of the Huize Giant Lead–Zinc Deposit, Yunnan, Province, China: Discussion on the Relationship Between the Emeishan Flood Basalts and Lead–Zinc Mineralization. Geological Publishing House, Beijing, pp. 1–214 (in Chinese).
Huang, Z.L., Li, X.B., Zhou, M.F., Li, W.B., Jin, Z.G., 2010. REE and C–O isotopic geochemistry of calcites from the word-class Huize Pb–Zn deposits, Yunnan, China: implication for the ore genesis. Acta Geol. Sin. (Engl. Ed.) 84, 597–613.
Huston, D.L., Sie, S.H., Suter, G.F., Cooke, D.R., Both, R.A., 1995. Trace elements in sulfide minerals from Eastern Australian volcanic-hosted massive sulfide deposits:

part 1. Proton microprobe analyses of pyrite, chalcopyrite, and sphalerite, and Part 2. Selenium levels in pyrite: comparison with $\delta^{34}S$ values and implications for the source of sulfur in volcanogenic hydrothermal systems. Econ. Geol. 90, 1167–1196.

Jin, Z.G., 2008. The Ore-control Factors, Ore-forming Regularity and Forecasting of Pb–Zn Deposit, in Northwestern Guizhou Province. Engine Industry Press, Beijing, pp. 1–105 (in Chinese).

Jorgenson, B.B., Isaksen, M.F., Jannasch, H.W., 1992. Bacterial sulfate reduction above 100 °C in deep sea hydrothermal vent sediments. Science 258, 1756–1757.

Leach, D.L., Sangster, D.F., 1993. Mississippi valley-type lead-zinc deposit. In: Kirkham, R.V., Sinclair, W.D., Thorpe, R.I., Duke, J.M. (Eds.), Mineral Deposit Modeling: Geological Association of Canada, Spe. Papers 40, pp. 289–314.

Leach, D.L., Sangster, D.F., 1996. Mississippi Valley-type lead–zinc deposits. In: Kirkham, R.V., Sinclair, W.D., Thorpe, R.I., Duke, J.M. (Eds.), Mineral Deposit Modeling: Geological Association of Canada Special Paper 40, pp. 289–314.

Leach, D.L., Bradley, D., Lewchuk, M.T., Symons, D.T.A., de Marsily, G., Brannon, J., 2001. Mississippi Valleytype lead–zinc deposits through geological time — implications from recent age-dating research. Miner. Deposita 36, 711–740.

Leach, D.L., Macquar, J.C., Lagneau, V., Leventhal, J., Emsbo, P., Premo, W., 2006. Precipitation of lead–zinc ores in the Mississippi Valley type deposit at Trèves, Cévennes region of southern France. Geofluids 6, 24–44.

Leach, D.L., Bradley, D.C., Huston, D., Pisarevsky, S.A., Taylor, R.D., Gardoll, S.J., 2010. Sediment-hosted lead–zinc deposits in Earth history. Econ. Geol. 105, 593–625.

Li, F.H., Qin, J.M., 1988. Presinian System in Kangdian Area. Chongqing Press, Chongqing, pp. 15–45 (in Chinese).

Li, L.J., Liu, H.T., Liu, J.S., 1999. A discussion on the source bed of Pb–Zn–Ag deposits in northeast Yunnan. Geol. Explor. NonFerrous Met. 8, 333–339 (in Chinese with English abstract).

Li, Q.L., Chen, F.K., Wang, X.L., Li, C.F., 2005. Ultra-low procedural blank and the single grain mica Rb–Sr isochron dating. Chin. Sci. Bull. 50, 2861–2865.

Li, W.B., Huang, Z.L., Yin, M.D., 2007a. Dating of the giant Huize Zn–Pb ore field of Yunnan province, southwest China: constraints from the Sm–Nd system in hydrothermal calcite. Resour. Geol. 57, 90–97.

Li, W.B., Huang, Z.L., Yin, M.D., 2007b. Isotope geochemistry of the Huize Zn–Pb ore field, Yunnan province, Southwestern China: implication for the sources of ore fluid and metals. Geochem. J. 41, 65–81.

Li, Q.L., Chen, F.K., Yang, J.H., Fan, H.R., 2008. Single grain pyrite Rb–Sr dating of the Linglong gold deposit, eastern China. Ore Geol. Rev. 34, 263–270.

Liao, W., 1984. A discussion on the S and Pb isotopic composition characteristics and metallogenic model of the Pb–Zn ore zones in eastern Yunnan and western Guizhou. J. Geol. Explor. 1, 1–6 (in Chinese with English abstract).

Lin, Z.Y., Wang, D.H., Zhang, C.Q., 2010. Rb–Sr isotopic age of sphalerite from the Paoma lead–zinc deposit in Sichuan Province and its implications. Geol. China 37, 488–494 (in Chinese with English abstract).

Liu, H.C., Lin, W.D., 1999. Study on the law of Pb–Zn–Ag Ore Dposit in Northeast Yunnan, China. Yunnan University Press, Kunming, pp. 1–468 (in Chinese).

Liu, H.Y., Xia, B., Zhang, Y.Q., 2004. Zircon SHRIMP dating of sodium alkaline rocks from Maomaogou area of Huili County in Panxi, SW China and its geological implications. Chin. Sci. Bull. 49, 1750–1756.

Machel, H.G., 1989. Relationships between sulphate reduction and oxidation of organic compounds to carbonate diagenesis, hydrocarbon accumulations, salt domes, and metal sulphide deposits. Carbonates Evaporites 4, 137–151.

Mao, D.M., 2000. Oxygen and carbon isotope in Guizhou Tianqiao Pb–Zn deposit. J. Guizhou Univ. Technol. 29, 8–11 (in Chinese with English abstract).

Mao, J.Q., Zhang, Q.H., Gu, S.Y., 1998. Tectonic Evolution and Pb–Zn Mineralization of Shuicheng Fault Subsidence. Guizhou Science and Technology Publishing Company, Guiyang, pp. 104–129 (in Chinese).

Mao, D.M., He, J.J., Liao, C.G., 2001. Sedimentary-reformation metallogenic characteristics of the Tianqiao lead–zinc deposit. Geol. Geochem. 29, 21–27 (in Chinese with English abstract).

Nakai, S., Halliday, A.N., Kesler, S.E., Jones, H.D., Kyle, J.R., Lanes, T.E., 1993. Rb–Sr dating of sphalerite from Mississippi Valley-type (MVT) ore deposits. Geochim. Cosmochim. Acta 57, 417–427.

Ohmoto, H., 1972. Systematics of sulfur and carbon isotopes in hydrothermal ore deposits. Econ. Geol. 67, 551–579.

Ohmoto, H., Goldhaber, M.B., 1997. Sulfur and carbon isotopes, In: Barnes, H.L. (Ed.), Geochemistry of Hydrothermal Ore Deposits, 3rd ed Wiley, New York, pp. 517–611.

Ohmoto, H., Kaiser, C.J., Geer, K.A., 1990. Systematics of sulphur isotopes in recent marine sediments and ancient sediment-hosted base metal deposits. In: Herbert, H.K., Ho, S.E. (Eds.), Stable Isotopes and Fluid Processes in Mineralisation: Geol Dep Univ Extens Univ Western Australia, 23, pp. 70–120.

Ottaway, T.L., Wicks, F.J., Bryndzia, L.T., 1994. Formation of the Muzo hydrothermal deposit in Colombia. Nature 369, 552–554.

Pfaff, K., Hildebrandt, L.H., Leach, D.L., Jacob, D.E., Markl, G., 2010. Formation of the Wiesloch Mississippi Valley-type Zn–Pb–Ag deposit in the extensional setting of the Upper Rhinegraben, SW Germany. Miner. Deposita 45, 647–666.

Qiu, Y.M., Gao, S., McNaughton, N.J., Groves, D.I., Ling, W.L., 2000. First evidence of >3.2 Ga continental crust in the Yangtze craton of south China and its implications for Archean crustal evolution and Phanerozoic tectonics. Geology 28, 11–14.

Recio, S.C., Fanlo, I., Fernández–Nieto, C., 1997. Stable isotope composition of F–Pb–Zn mineralization in the Valle de Tena (Spanish Central Pyrenees). Miner. Deposita 32, 180–188.

Reid, A., Wilson, C.J.L., Shun, L., Pearson, N., Belousova, E., 2007. Mesozoic plutons of the Yidun Arc, SW China: U/Pb geochronology and Hf isotopic signature. Ore Geol. Rev. 31, 88–106.

Sangster, D.F., 1983. Mississippi Valley-type deposits: a geological mélange. In: Kisvarsanyi, G., Grant, S.K., Pratt, W.P., Koenig, J.W. (Eds.), Proceedings of International Conference on Mississippi Valley-type Lead–Zinc Deposits. University of Missouri–Rolla Press, Rolla, MO, pp. 7–19.

Sangster, D.F., 1996. Mississippi Valley-type lead–zinc. In: Types, O.R., Sinclair, E.W.D., Thorpe, R.I. (Eds.), Geology of Canadian Mineral Deposit: Geological Survey of Canada, Geology of Canada, 8, pp. 253–261.

Seal, I.R., 2006. Sulfur isotope geochemistry of sulfide minerals. Rev. Mineral. Geochem. 61, 633–677.

Sun, W.H., Zhou, M.F., Yan, D.P., Li, J.W., Ma, Y.X., 2008. Provenance and tectonic setting of the Neoproterozoic Yanbian Group, western Yangtze Block (SW China). Precambrian Res. 167, 213–236.

Sun, W.H., Zhou, M.F., Gao, G.F., Yang, Y.H., Zhao, X.F., Zhao, J.H., 2009. Detrital zircon U–Pb geochronological and Lu–Hf isotopic constraints on Detrital zircon U–Pb geochronological and Lu–Hf isotopic constraints on the Precambrian magmatic and crustal evolution of the western Yangtze Block, SW China. Precambrian Res. 172, 99–126.

Tu, G.Z., 1984. Geochemistry of Strata-bound Ore Deposits in China (Volumes I). Science Press, Beijing, pp. 13–69 (in Chinese with English abstract).

Wang, H.Y., 1993. Geochemistry of Pb–Zn mineralization in Guizhou. Guizhou Geol. 10, 272–290 (in Chinese with English abstract).

Wang, L.J., 1994. Geological and geochemical features of lead–zinc deposits in northwestern, Guizhou Province, China. J. Guilin Coll. Geol. 14, 125–130 (in Chinese with English abstract).

Wang, H.Y., Liang, F.L., Zeng, D.Q., 1996. Geology of the Pb–Zn Deposits in Guizhou Province. Guizhou Technological Publishing House, Guiyang, pp. 1–231 (in Chinese with English abstract).

Wang, X.C., Zheng, Z.R., Zheng, M.H., Xu, X.H., 2000. Metallogenic mechanism of the Tianbaoshan Pb–Zn deposit, Sichuan. Chin. J. Geochem. 19, 121–133.

Wang, J.Z., Li, Z.Q., Ni, S.J., 2003. Origin of ore-forming fluids of Mississippi Valley-type (MVT) Pb–Zn deposits in Kangdian area, China. Chin. J. Geochem. 22, 369–376.

Wang, C.M., Deng, J., Zhang, S.T., Xue, C.J., Yang, L.Q., Wang, Q.F., Sun, X., 2010. Sediment-hosted Pb–Zn deposits in southwest Sanjiang Tethys and Kangdian area on the western margin of Yangtze Craton. Acta Geol. Sin. (Engl. Ed.) 84, 1428–1438.

Wang, W., Zhou, M.F., Yan, D.P., Li, J.W., 2012. Depositional age, provenance, and tectonic setting of the Neoproterozoic Sibao Group, southeastern Yangtze Block, South China. Precambrian Res. 192, 107–124.

Wilkinson, J.J., Eyre, S.L., Boyce, A.J., 2005. Ore-forming processes in Irish-type carbonate-hosted Zn–Pb deposits: evidence from mineralogy, chemistry, and isotopic composition of sulfides at the Lisheen Mine. Econ. Geol. 100, 63–86.

Worden, R.H., Smalley, P.C., Oxtoby, N.H., 1995. Gas souring by the thermochemical sulfate reduction at 140 °C. AAPG Bull. 79, 854–863.

Xie, J.R., 1963. Introduction of the Chinese Ore Deposits. Scientific books Publishing House, Beijing, pp. 1–71 (in Chinese).

Yan, D.P., Zhou, M.F., Song, H.L., Wang, X.W., Malpas, J., 2003. Origin and tectonic significance of a Mesozoic multi-layer over-thrust system within the Yangtze Block (South China). Tectonophysics 361, 239–254.

Yan, Z.F., Huang, Z.L., Xu, C., Chen, M., Zhang, Z.L., 2007. Signatures of the source for the Emeishan flood basalts in the Ertan area: Pb isotope evidence. Chin. J. Geochem. 26, 207–213.

Yin, M.D., Li, W.B., Sun, X.W., 2009. Rb–Sr isotope dating of sphalerite from the giant Huize Zn–Pb ore field Yunnan province, southwestern China. Chin. J. Geochem. 28, 70–75.

Zartman, R.E., Doe, B.R., 1981. Plumbotectonics—the model. Tectonophysics 75, 135–162.

Zhang, Y.X., Luo, Y.N., Yang, C.X., 1988. Panzhihua–Xichang Rift in China. Geological Publishing House, Beijing, pp. 290–297 (in Chinese).

Zhang, Q.H., Mao, J.Q., Guang, S.Y., 1998. The studies of ore-forming material sources of metal deposit in Hezhang Pb–Zn mine Shuicheng, Guizhou province. J. Guizhou Univ. Technol. 27, 26–34 (in Chinese with English abstract).

Zhang, Z.B., Li, C.Y., Tu, G.C., Xia, B., Wei, Z.Q., 2006. Geotectonic evolution background and ore-forming process of Pb–Zn deposits in Chuan–Dian–Qian area of southwest China. Geotecton. Metallog. 30, 343–354 (in Chinese with English abstract).

Zhang, C.Q., Li, X.H., Yu, J.J., Mao, J.W., Chen, F.K., Li, H.M., 2008. Rb–Sr dating of single sphalerite from the Daliangzi Pb–Zn deposit, Sichuan, and its geological significances. Geol. Rev. 54, 533–538 (in Chinese with English abstract).

Zhao, X.F., Zhou, M.F., Li, J.W., Sun, M., Gao, J.F., Sun, W.H., Yang, J.H., 2010. Late Paleoproterozoic to early Mesoproterozoic Dongchuan Group in Yunnan, SW China: implications for tectonic evolution of the Yangtze Block. Precambrian Res. 182, 57–69.

Zheng, C.L., 1994. An approach on the source of ore-forming metals of lead–zinc deposits in Northwestern part, Guizhou, Province. J. Guilin Coll. Geol. 14, 113–124 (in Chinese with English abstract).

Zheng, M.H., Wang, X.C., 1991. Genesis of the Daliangzi Pb–Zn deposit in Sichuan, China. Econ. Geol. 86, 831–846.

Zhou, C.X., Wei, C.S., Guo, J.Y., 2001. The source of metals in the Qilingchang Pb–Zn deposit, Northeastern Yunnan, China: Pb–Sr isotope constraints. Econ. Geol. 96, 583–598.

Zhou, M.F., Malpas, J., Song, X.Y., Robinson, P.T., Sun, M., Kennedy, A.K., Lesher, C.M., Keays, R.R., 2002a. A temporal link between the Emeishan large igneous province (SW China) and the end—Guadalupian mass extinction. Earth Planet. Sci. Lett. 196, 113–122.

Zhou, M.F., Yan, D.P., Kennedy, A.K., Li, Y.Q., Ding, J., 2002b. SHRIMP zircon geochronological and geochemical evidence for Neo-proterozoic arc-related magmatism along the western margin of the Yangtze Block, South China. Earth Planet. Sci. Lett. 196, 1–67.

Zhou, M.F., Arndt, N.T., Malpas, J., Wang, C.Y., Kennedy, A., 2008. Two magma series and associated ore deposit types in the Permian Emeishan large igneous province, SW China. Lithos 103, 352–368.

Zhou, J.X., Huang, Z.L., Zhou, G.F., Jin, Z.G., Li, X.B., Ding, W., Gu, J., 2010a. Sources of the ore metals of the Tianqiao Pb–Zn deposit in northwestern Guizhou province: constraints form S, Pb isotope and REE geochemistry. Geol. Rev. 56, 513–524 (in Chinese with English abstract).

Zhou, J.X., Huang, Z.L., Zhou, G.F., Li, X.B., Ding, W., Bao, G.P., 2010b. Sulfur isotopic compositions of the Tianqiao Pb–Zn ore deposit, Guizhou Province, China: implications for the source of sulfur in the ore-forming fluids. Chin. J. Geochem. 29, 301–306.

Zhou, J.X., Huang, Z.L., Zhou, G.F., Li, X.B., Ding, W., Bao, G.P., 2011. Trace elements and rare earth elements of sulfide minerals in the Tianqiao Pb–Zn Ore deposit, Guizhou province, China. Acta Geol. Sin. (Engl. Ed.) 85, 189–199.